Latin American Journal of Solids and Structures
www.lajss.org

Free Damped Vibration of Rotating Truncated Conical Sandwich Shells Using an Improved High-Order Theory

Abstract

In the present paper, an improved high-order theory is employed to study the free vibration of rotating truncated sandwich conical shells with laminated face sheets and a soft core. The formulation is based on a three-layer sandwich model. First-order shear deformation theory (FSDT) is used for face sheets and quadratic and cubic functions are assumed for transverse and in-plane displacements of the core, respectively. The governing equations of motion are derived according to the Hamilton's principle. Also, continuity conditions of the displacements at the interfaces, as well as transverse flexibility, transverse normal strain and stress of the core have been considered. Analytical solution for free vibration of simply supported sandwich conical shells is presented using Galerkin's method. Effect of some geometrical parameters is also studied on the fundamental frequency of the sandwich shells. Comparison of the present results with those in the literature confirms the accuracy of the proposed theory.

Keywords

Rotating conical shell, high-order sandwich theory, free vibration.

Amir Shekari [a, *]
Faramarz Ashenai Ghasemi [b]
Keramat Malekzadehfard [c]

[a] Phd student of Mechanical Engineering, Shahid Rajaee Teacher Training University, Tehran, Iran, ar.shekari@gmail.com,
[b] Faculty of Mechanical Engineering, Shahid Rajaee Teacher Training University, Tehran, Iran, f.a.ghasemi@srttu.edu faramarz_ashenai_ghasemi@yahoo.com
[c] Department of Structural Analysis and Simulation, Aerospace Research Institute, Malek Ashtar University of Technology, Tehran, Iran, k.malekzadeh@gmail.com

* Corresponding author

http://dx.doi.org/10.1590/1679-78253977

Received 29.04.2017
In revised form 23.08.2017
Accepted 27.08.2017
Available online 18.09.2017

1 INTRODUCTION

One of the most widely used shell structures in the aerospace, aeronautic and other engineering applications and industries such as nuclear fuels, petrochemical, submarine hulls, hoppers, vessel heads, component of flying objects and space crafts is the shell of revolution especially in the forms

of truncated conical shells and different shell theories have been presented to considering the shear deformation behaviors. Most studies on these specific geometries have been limited to those with uniform equivalent layer with isotropic, orthotropic and laminated composite materials or FGMs, which has been of considerable interest over the past few years. For shells having a small thickness, a first order shear deformation theory (FSDT) is good to consider the effects of rotary inertia and transverse shear deformation but for thick shells especially those with thickness variation using a high order shear deformation theory is inevitable (Amabili and Reddy, 2010- Amabili, 2013).
Sandwich structures with laminated face sheets are recognized for high-structural efficiency and are used widely in different applications. These structures have been restrictively applied due to the lack of sufficient information about dynamic behavior. These panels are usually contained of two tough face sheets and a soft core, which are connected together. Usually, the core is contained of a soft and thick material, when thin composite laminates are mostly employed as the face sheets. The core holds the face plates at adequate space and transmits the loads. Therefore, there will be a great bending stiffness and an excellent low weight. To date, there have been many efforts to understand the mechanical behavior of sandwich panels and multiple theories have been proposed. These are the 3D elasticity theory as in Kardomateas (2005)-Ji et al. (2010), equivalent single layer (ESL) theories (Kant and Swaminathan, 2002- Matsunaga, 2005- Nayak et al., 2006), global-local theories (Shariyat, 2012) and layer-wise (LW) theories (Frostig et al., 1992). Most of the studies on sandwich analysis using these theories have been performed in static and buckling analysis fields. The LW theories expand the separate displacement field expansions through each layer. Because of capability of the LW theories, the development of accurate sandwich shell theories has been the subject of significant research interest for many years. Noor et al. (1996) have classified sandwich structures from simple beams to doubly curved shells. A comparison of different models for soft core sandwich structures has been given by Carrera and Brischetto (2009). Higher order sandwich panel (HSPT) theories are needed for thick sandwich shells. New sandwich structures are mostly manufactured from two laminated face sheets and a soft material core. Cores are mostly thick and transformative in all directions. This leads to unknown deformation patterns particularly through the thickness of the structure. Also, the thin or moderately thick face sheets of the sandwich structure show various displacement patterns, thus the displacements of the upper and lower face sheets may be different from each other (Reddy, 2004). These effects cannot be exactly specified by classical sandwich theories.

To study the effect of thickness and compressibility of the core, different theories have been expanded (see for example Frostig et al., 1992 and Malekzadeh, 2005). In some of these theories, the core is noted as a linear elastic material that has only vertical and shear stiffness and its longitudinal stresses are omitted (Frostig et al., 1992). In the improved high-order theories such as the model presented by Malekzadeh et al. (2005), the longitudinal stresses in the core have been considered and successfully used to study different problems of these structures especially in vibration cases. However, only a few researches on sandwich structures have investigated the coordinate in thickness direction to radius of curvature ratio effect in formulation (Malekzadeh and Livani, 2015).

More works are focused on sandwich beams, plates and to some extents, cylindrical and doubly curved shells compared with the conical shell, and just a few researchers have tried to deal with free vibration analysis of sandwich conical shells with three distinct layers. Free vibrations of orthotropic

sandwich shells of revolution have been done by Bacon and Bert (1962) and Bert and Ray (1969). Wilkins et al. (1970) studied the free vibrations of sandwich conical shells with different boundary conditions. The first-approximation shell theory of Love, with transverse shear strain added, was applied and solutions were acquired by Galerkin's method. Gupta and Jain (1978) discussed the axisymmetric free vibration of truncated conical sandwich shells applying FSDT and Rayleigh-Ritz procedure. A specific finite element method was expanded by Ramesh and Ganesan (1994) to investigate the vibration specifications of some conical shells. By using a finite element method, Bardell et al. (1999) presented an efficient approach to analyze the vibration of sandwich conical shells. Korjakin et al. (2001), investigated the free damped vibrations of sandwich shells of revolution. Zhong and Reimerdes (2007) used a higher-order theory to investigate the buckling of cylindrical and conical sandwich shells having a flexible core. They applied the Kirchhoff–Love theory for the face plates and omitted in-plane extensional and shear stiffness of the core. By using Fourier decomposition, they solved the problem through a numerical integration procedure.

Sharnappa et al. (2009) presented free vibration analysis of truncated sandwich conical shells with ER fluid core. Malekzadeh and Livani (2015) performed the buckling analysis of a truncated conical composite sandwich panel with different boundary conditions. Seidi et al. (2015) studied the buckling of a sandwich truncated conical shell. They used a high order theory for modeling sandwich shells, in which FSDT has been used for modeling the displacements in thin FG face sheets and cubic functions for core. Mozaffari and Morovat (2015) studied the buckling of laminated composite truncated conical sandwich shells with flexible core subject to combine axial compressive load and external pressure

On the other hand, rotating conical structures are extensively used in many mechanical and aerospace applications, such as in high-speed centrifugal separators, drive shafts of advanced gas turbines, high-power aircraft jet engines, motors and rotor systems. The free vibration analysis of rotating truncated conical shells has been carried out extensively in previous works as in Lam and Hua (1999a,b) and (2000a,b,c), Civalek (2006) and Dey and Karmakar (2012). Lam and Hua (1997), based upon Love's first approximation theory, presented a dynamic model for the rotating truncated circular conical shells. Chen et al. (1993) studied the effects of Coriolis and large deformations on free vibration of a rotating shell of revolution.

Using relatively thick shell theory, Sivadas (1995) studied the frequencies of a pre-stressed rotating conical shell. Lam and Hua (1999b) provided an approach to discuss the free vibration of a rotating circular orthotropic conical shell. Hua (2000c) also studied the effect of boundary conditions on the vibration specifications of a rotating multilayered conical shell. In another study, Lam and Hua (2001) calculated frequencies of a truncated circular rotating conical shell. By using the generalized differential quadrature (GDQ) method, Ng et al. (2003) presented the orthotropic influence of composite materials on frequency specifications for a rotating thin truncated circular symmetrical composite conical shell. Hua et al. (2005) wrote a worthwhile book in this area.

Based upon the model of Lam and Hua (1997), Civalek (2006) presented an approach to study the free vibration of rotating truncated conical shells. He used discrete singular convolution (DSC) method to calculate frequencies of an isotropic conical shell. Recently, Chen and Dai (2009) and Chen (2012) studied the nonlinear vibration of a rotating truncated conical shell. Talebitooti et al. (2010), using an energy-based approach, presented an analytical solution for the free vibration of rotating composite conical shells with axial and circumferential stiffeners. Talebitooti (2013) also studied free

vibration of thick, rotating composite conical shells based on the 3D theory, using the layer-wise differential quadrature method (LW-DQM). Qinkai and Fulei (2013) offered a modified approach for rotating truncated conical shells. The instability behaviors of rotating truncated conical shells were analyzed by Han and Chu (2013), who reported the rotating speed to be constant and the instability to be induced by the periodic axial loads.

Malekzadeh and Heydarpour (2013) studied the free vibration of rotating FG truncated conical shells. Heydarpour et al. (2014) presented the free vibration of rotating functionally graded composite truncated conical shells. They used the FSDT theory and DQM method to study the free vibration. Han and Chu (2014) studied resonance of truncated conical shells. They used the improved Hill's method for parametric instability analysis. However, a thorough search of the relevant literature revealed that the free vibration behavior of the rotating sandwich truncated conical shells with three distinct layers and flexible core has not yet been investigated and just a few studies were presented on frequency analysis of rotating sandwich conical shells with isotropic layers, an example of which could be in book written by Hua et al. (2005).

Here, an improved high-order sandwich panel theory is employed to investigate the free vibration of a rotating truncated sandwich conical panel with composite faces and homogenous soft core for the first time, considering the effect of thickness to radius of curvature ratio. The first-order shell assumptions are applied to the face sheets, and cubic and quadratic functions are presumed for the in-plane and transverse displacements of the core, respectively. Continuity conditions of the displacements at the interfaces are satisfied. Also, transverse flexibility as well as transverse normal strain and stress of the core are considered. The equations of motion and boundary conditions are derived via the Hamilton's principle. Analytical solution is presented for free vibration analysis of simply supported rotating sandwich truncated conical shells. The system of partial differential equations is simplified to an ordinary one. The effects of some geometrical parameters are also studied.

2 GEOMETRY

As shown in Figure 1, a truncated conical sandwich shell is considered, which rotates about its symmetrical axis with a constant angular velocity Ω. This system is mentioned to as a curvilinear coordinate system (s, ϑ, z), where s and ϑ axes are along the generator and in the circumferential direction on the reference surface of the cone, respectively, and the z-axis, is perpendicular to the plane of the first two axes, lies in the outwards normal direction of the cone. Also, in Figure 1, r indicates the radii of the cone normal to the axis of symmetry; β shows the semi-vertex angle of the cone and h_c, h_o and h_i are the core, outer and inner face sheet thicknesses, respectively. The materials of the face sheets are considered to be laminated composite, and the core is considered homogeneous. R_ϑ is the core radius in the thickness direction. Thus:

$$\mathrm{R}_\theta = \mathrm{s} \cdot \tan\beta \tag{1}$$

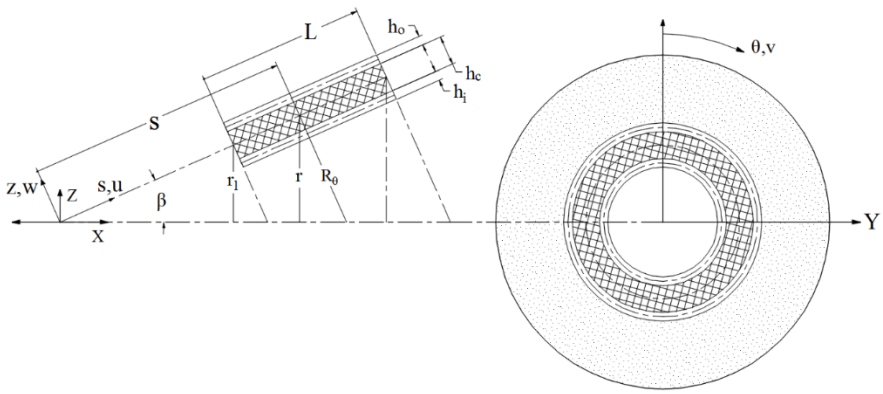

Figure 1: Geometrical parameters of a rotating truncated conical sandwich shell.

3 MATHEMATICAL FORMULATION

3.1 Kinematic Relations

Here, FSDT is adopted for the face sheets as:

$$\begin{cases} u_j(s,\theta,z_j) = u_{0j}\left(s,\theta\right) + z_j\varphi_s^j\left(s,\theta\right) \\ v_j(s,\theta,z_j) = (1+\dfrac{z_j}{R_\theta^j})v_{0j}\left(s,\theta\right) + z_j\varphi_\theta^j\left(s,\theta\right) \\ w_j(s,\theta,z_j) = w_j\left(s,\theta\right) \end{cases} \quad , \quad j=(o,i) \tag{2}$$

where u_0, v_0 and w_0 are the displacements of the mid-surface along the s, ϑ and z direction and φ_s^j and φ_ϑ^j are the rotations of the normal to the mid-surface along the s and ϑ axis, respectively. Because, the core layer is thicker and softer than the face sheet, the displacement fields for the core are assumed to be cubic and have quadratic pattern for the in-plane and out-of-plane displacement components, respectively (Malekzadeh and Livani, 2015):

$$\begin{cases} u_c\left(s,\theta,z_c\right) = u_0\left(s,\theta\right) + u_1\left(s,\theta\right)z_c + u_2\left(s,\theta\right)z_c^{\,2} + u_3\left(s,\theta\right)z_c^{\,3} \\ v_c\left(s,\theta,z_c\right) = (1+\dfrac{z_c}{R_\theta^c})v_0\left(s,\theta\right) + v_1\left(s,\theta\right)z_c + v_2\left(s,\theta\right)z_c^{\,2} + v_3\left(s,\theta\right)z_c^{\,3} \\ w_c\left(s,\theta,z_c\right) = w_0\left(s,\theta\right) + w_1\left(s,\theta\right)z_c + w_2\left(s,\theta\right)z_c^{\,2} \end{cases} \tag{3}$$

where u_k and v_k (k = 0, 1, 2, 3) are the unknowns of the in-plane displacement components of the core and w_k(k = 0, 1, 2) are the unknowns of its vertical displacements, respectively. Here, there are 27 unknowns: ten displacement unknowns for both the face sheets, eleven displacement unknowns for the core, and six Lagrange multipliers.

3.2 Compatibility Conditions

Here, the core is completely bonded to the face sheets. Therefore, there are three interface displacements in each face sheet-core interface, which can be obtained as follows:

$$
\begin{aligned}
&u_o\left(z_o=-h_o/2\right)=u_c\left(z_c=h_c/2\right); \quad v_o\left(z_o=-h_o/2\right)=v_c\left(z_c=h_c/2\right);\\
&w_o\left(z_o=-h_o/2\right)=w_c\left(z_c=h_c/2\right)\\
&u_i\left(z_i=h_i/2\right)=u_c\left(z_c=-h_c/2\right); \quad v_i\left(z_i=h_i/2\right)=v_c\left(z_c=-h_c/2\right);\\
&w_i\left(z_i=h_i/2\right)=w_c\left(z_c=-h_c/2\right)
\end{aligned}
\tag{4}
$$

3.3 Strain Components

The strain–displacement relations for the face sheets (j=o, i) are:

$$
\begin{aligned}
\varepsilon_{ss}^{j} &= u_{0j,s}+z_j\varphi_{s,s}^{j}\\
\varepsilon_{\theta\theta}^{j} &= \frac{1}{r_j}\left((1+\frac{z_j}{R_\theta^j})v_{0j,\theta}+z_j\varphi_{\theta,\theta}^{j}+u_{0j}\cdot sin\beta+z_j\varphi_s^j\cdot sin\beta+w_j\cdot cos\beta\right)\\
\varepsilon_{zz}^{j} &= 0 \qquad , \qquad j=\left(o,i\right)\\
\varepsilon_{s\theta}^{j} &= (1+\frac{z_j}{R_\theta^j})v_{0j,s}+z_j\varphi_{\theta,s}^{j}\\
\varepsilon_{\theta s}^{j} &= \frac{1}{r_j}(u_{0j,\theta}+z_j\varphi_{s,\theta}^{j}-(1+\frac{z_j}{R_\theta^j})v_{0j}\cdot sin\beta-z_j\varphi_\theta^j\cdot sin\beta)\\
\gamma_{s\theta}^{j} &= \varepsilon_{s\theta}^{j}+\varepsilon_{\theta s}^{j}=\frac{1}{r_j}(r_j((1+\frac{z_j}{R_\theta^j})v_{0j,s}+z_j\varphi_{\theta,s}^{j})+u_{0j,\theta}+z_j\varphi_{s,\theta}^{j}-(1+\frac{z_j}{R_\theta^j})v_{0j}\cdot sin\beta\\
&\quad -z_j\varphi_\theta^j\cdot sin\beta)\\
\gamma_{sz}^{j} &= \varphi_s^j+w_{j,s}\\
\gamma_{\theta z}^{j} &= \frac{1}{r_j}(w_{j,\theta}-(1+\frac{z_j}{R_\theta^j})v_{0j}\cdot cos\beta-z_j\varphi_\theta^j\cdot cos\beta)+\frac{1}{R_\theta^j}v_{0j}+\varphi_\theta^j
\end{aligned}
\tag{5}
$$

The strain–displacement relations for the core are:

$$
\begin{aligned}
\varepsilon_{ss}^{c} &= u_{0,s}+u_{1,s}z_c+u_{2,s}{z_c}^2+u_{3,s}{z_c}^3\\
\varepsilon_{\theta\theta}^{c} &= \frac{1}{r_c}[(1+\frac{z_c}{R_\theta^c})v_{0,\theta}+v_{1,\theta}z_c+v_{2,\theta}{z_c}^2+v_{3,\theta}{z_c}^3+\left(u_0+u_1z_c+u_2{z_c}^2+u_3{z_c}^3\right)\sin\beta\\
&+\left(w_0+w_1z_c+w_2{z_c}^2\right)\cos\beta]\\
\varepsilon_{zz}^{c} &= w_1+2w_2z_c\\
\varepsilon_{s\theta}^{c} &= -(\frac{tg\beta z_c}{R_\theta^{c2}})v_0+(1+\frac{z_c}{R_\theta^c})v_{0,s}+v_{1,s}z_c+v_{2,s}{z_c}^2+v_{3,s}{z_c}^3\\
\varepsilon_{\theta s}^{c} &= \frac{1}{r_c}(u_{0,\theta}+u_{1,\theta}z_c+u_{2,\theta}{z_c}^2+u_{3,\theta}{z_c}^3-((1+\frac{z_c}{R_\theta^c})v_0+v_1z_c+v_2{z_c}^2+v_3{z_c}^3)\sin\beta)\\
\gamma_{s\theta}^{c} &= \varepsilon_{s\theta}^{c}+\varepsilon_{\theta s}^{c}\\
\gamma_{sz}^{c} &= (u_1+2u_2z_c+3u_3{z_c}^2)+(w_{0,s}+w_{1,s}z_c+w_{2,s}{z_c}^2)\\
\gamma_{\theta z}^{c} &= \frac{1}{r_c}(w_{0,\theta}+w_{1,\theta}z_c+w_{2,\theta}{z_c}^2-((1+\frac{z_c}{R_\theta^c})v_0+v_1z_c+v_2{z_c}^2+v_3{z_c}^3)\cos\beta)\\
&+(\frac{1}{R_\theta^c})v_0+v_1+2v_2z_c+3v_3{z_c}^2
\end{aligned}
\tag{6}
$$

in which $r_j=(R\vartheta^j+z_j)\cos\beta$ for (j=o, i, c).

3.4 Stress Resultants

To determine the stress resultants for each face sheet, constitutive equations can be written as follows (Figure 2):

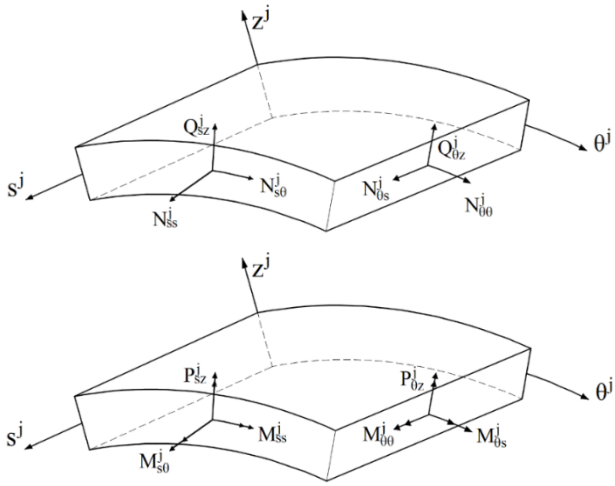

Figure 2: Stress and moment resultants of the face sheets.

$$\begin{Bmatrix} N^j_{ss} \\ N^j_{s\theta} \\ Q^j_{sz} \end{Bmatrix} = \int_{-\frac{h_j}{2}}^{\frac{h_j}{2}} \begin{Bmatrix} \sigma^j_{ss} \\ \tau^j_{s\theta} \\ \tau^j_{sz} \end{Bmatrix} (1 + \frac{z_j}{R^j_\theta}) dz_j, \qquad \begin{Bmatrix} M^j_{ss} \\ M^j_{s\theta} \\ P^j_{sz} \end{Bmatrix} = \int_{-\frac{h_j}{2}}^{\frac{h_j}{2}} \begin{Bmatrix} \sigma^j_{ss} \\ \tau^j_{s\theta} \\ \tau^j_{sz} \end{Bmatrix} (1 + \frac{z_j}{R^j_\theta}) \, z_j \, .dz_j$$

$$\begin{Bmatrix} N^j_{\theta\theta} \\ N^j_{\theta s} \\ Q^j_{\theta z} \\ N^j_{zz} \end{Bmatrix} = \int_{-\frac{h_j}{2}}^{\frac{h_j}{2}} \begin{Bmatrix} \sigma^j_{\theta\theta} \\ \tau^j_{s\theta} \\ \tau^j_{\theta z} \\ \sigma^j_{zz} \end{Bmatrix} dz_j, \qquad \begin{Bmatrix} M^j_{\theta\theta} \\ M^j_{\theta s} \\ P^j_{\theta z} \\ M^j_{zz} \end{Bmatrix} = \int_{-\frac{h_j}{2}}^{\frac{h_j}{2}} \begin{Bmatrix} \sigma^j_{\theta\theta} \\ \tau^j_{s\theta} \\ \tau^j_{\theta z} \\ \sigma^j_{zz} \end{Bmatrix} z_j .dz_j \tag{7}$$

$$\begin{bmatrix} N^j_{ss} \\ N^j_{\theta\theta} \\ N^j_{s\theta} \\ N^j_{\theta s} \\ N^j_{zz} \\ M^j_{ss} \\ M^j_{\theta\theta} \\ M^j_{s\theta} \\ M^j_{\theta s} \\ M^j_{zz} \end{bmatrix} = \begin{bmatrix} Ar_{11} & \frac{1}{B^j}A_{12} & \frac{1}{B^j}\bar{A}_{12} & Ar_{16} & \frac{1}{B^j}A_{16} & \frac{1}{B^j}A_{16} & Br_{11} & \frac{1}{B^j}B_{12} & Br_{16} & \frac{1}{B^j}B_{16} \\ A_{12} & \bar{A}_{22} & \hat{A}_{22} & A_{26} & \bar{A}_{26} & \bar{A}_{26} & B_{12} & \bar{B}_{22} & B_{26} & \bar{B}_{26} \\ Ar_{16} & \frac{1}{B^j}A_{26} & \frac{1}{B^j}\bar{A}_{26} & Ar_{66} & \frac{1}{B^j}A_{66} & \frac{1}{B^j}A_{66} & Br_{16} & \frac{1}{B^j}B_{26} & Br_{66} & \frac{1}{B^j}B_{66} \\ A_{16} & \bar{A}_{26} & \hat{A}_{26} & A_{66} & \bar{A}_{66} & \bar{A}_{66} & B_{16} & \bar{B}_{26} & B_{66} & \bar{B}_{66} \\ A_{31} & \bar{A}_{32} & \hat{A}_{32} & A_{36} & \bar{A}_{36} & \bar{A}_{36} & B_{31} & \bar{B}_{32} & B_{36} & \bar{B}_{36} \\ Br_{11} & \frac{1}{B^j}B_{12} & \frac{1}{B^j}\bar{B}_{12} & Br_{16} & \frac{1}{B^j}B_{16} & \frac{1}{B^j}B_{16} & Dr_{11} & \frac{1}{B^j}D_{12} & Dr_{16} & \frac{1}{B^j}D_{16} \\ B_{12} & \bar{B}_{22} & \hat{B}_{22} & B_{26} & \bar{B}_{26} & \bar{B}_{26} & D_{12} & \bar{D}_{22} & D_{26} & \bar{D}_{26} \\ Br_{16} & \frac{1}{B^j}B_{26} & \frac{1}{B^j}\bar{B}_{26} & Br_{66} & \frac{1}{B^j}B_{66} & \frac{1}{B^j}B_{66} & Dr_{16} & \frac{1}{B^j}D_{26} & Dr_{66} & \frac{1}{B^j}D_{66} \\ B_{16} & \bar{B}_{26} & \hat{B}_{26} & B_{66} & \bar{B}_{66} & \bar{B}_{66} & D_{16} & \bar{D}_{26} & D_{66} & \bar{D}_{66} \\ B_{31} & \bar{B}_{32} & \hat{B}_{32} & B_{36} & \bar{B}_{36} & \bar{B}_{36} & D_{31} & \bar{D}_{32} & D_{36} & \bar{D}_{36} \end{bmatrix} \times \begin{bmatrix} \varepsilon^j_{0ss} \\ \varepsilon^j_{0\theta\theta} \\ \varepsilon^j_{1\theta\theta} \\ \varepsilon^j_{0s\theta} \\ \varepsilon^j_{1s\theta} \\ \varepsilon^j_{0\theta s} \\ \kappa^j_{ss} \\ \kappa^j_{\theta\theta} \\ \varepsilon^j_{2s\theta} \\ \varepsilon^j_{1\theta s} \end{bmatrix} \tag{8}$$

$$\begin{bmatrix} Q_{sz}^{j} \\ Q_{\theta z}^{j} \\ P_{sz}^{j} \\ P_{\theta z}^{j} \end{bmatrix} = \begin{bmatrix} Ar_{55} & \frac{1}{B^{j}} A_{45} & \frac{1}{B^{j}} B_{45} & Ar_{55} \\ A_{45} & \overline{A}_{44} & \overline{B}_{44} & A_{44} \\ Br_{55} & \frac{1}{B^{j}} B_{45} & \frac{1}{B^{j}} D_{45} & Br_{45} \\ B_{45} & \overline{B}_{44} & \overline{D}_{44} & B_{44} \end{bmatrix} \times \begin{bmatrix} \gamma_{0sz}^{j} \\ \gamma_{0\theta z}^{j} \\ \gamma_{1\theta z}^{j} \\ \gamma_{2\theta z}^{j} \end{bmatrix} \tag{9}$$

Also, the stiffness matrices components for the outer and inner face sheets are as follows:

$$\begin{aligned}
&\begin{Bmatrix} A_{ij} \\ B_{ij} \\ D_{ij} \\ E_{ij} \end{Bmatrix} = K_i \times K_j \times \int_{-h_j/2}^{h_j/2} Q(i,j) \begin{Bmatrix} 1 \\ z_j \\ z_j^2 \\ z_j^3 \end{Bmatrix} \mathrm{d}\, z_j \quad , \quad (\mathrm{i,j} = 1..6) \\
&\begin{Bmatrix} Ar_{ij} \\ Br_{ij} \\ Dr_{ij} \end{Bmatrix} = K_i \times K_j \times \int_{-h_j/2}^{h_j/2} Q(i,j)(1 + \frac{z_j}{R_\theta^j}) \begin{Bmatrix} 1 \\ z_j \\ z_j^2 \end{Bmatrix} \mathrm{d}\, z_j \ , \ i,j = 1..6 \\
&\begin{Bmatrix} \overline{A}_{ij} \\ \overline{B}_{ij} \\ \overline{D}_{ij} \end{Bmatrix} = K_i \times K_j \times \int_{-h_j/2}^{h_j/2} Q(i,j) \frac{1}{r_j} \begin{Bmatrix} 1 \\ z_j \\ z_j^2 \end{Bmatrix} \mathrm{d}\, z_j \ , \ i,j = 1..6 \\
&\begin{Bmatrix} \hat{A}_{ij} \\ \hat{B}_{ij} \\ \hat{D}_{ij} \end{Bmatrix} = K_i \times K_j \times \int_{-h_j/2}^{h_j/2} Q(i,j) \frac{1}{r_j^2} \begin{Bmatrix} 1 \\ z_j \\ z_j^2 \end{Bmatrix} \mathrm{d}\, z_j \ , \ i,j = 1..6 \\
&K_i = K_j = \begin{cases} \pi^2 \ / \ 12 & for \quad (i,j = 4,5) \\ 1 & for \quad (i,j \neq 4,5) \end{cases}
\end{aligned} \tag{10}$$

where the strain components for a sandwich truncated conical shell are defined as:

$$\begin{bmatrix} \varepsilon_{0ss}^{j} \\ \varepsilon_{0\theta\theta}^{j} \\ \varepsilon_{1\theta\theta}^{j} \\ \varepsilon_{0s\theta}^{j} \\ \varepsilon_{1s\theta}^{j} \\ \varepsilon_{0\theta s}^{j} \\ \kappa_{ss}^{j} \\ \kappa_{\theta\theta}^{j} \\ \varepsilon_{2s\theta}^{j} \\ \varepsilon_{1\theta s}^{j} \end{bmatrix} = \begin{bmatrix} u_{0j,s} \\ v_{0j,\theta} + u_{0j} \cdot sin\beta + w_j \cdot cos\beta \\ 0 \\ v_{0j,s} \\ 0 \\ u_{0j,\theta} - v_{0j} \cdot sin\beta \\ \varphi_{s,s}^{j} \\ \frac{1}{R_\theta^j} v_{0j,\theta} + \varphi_{\theta,\theta}^{j} + \varphi_s^j \cdot sin\beta \\ \frac{1}{R_\theta^j} v_{0j,s} + \varphi_{\theta,s}^{j} \\ \varphi_{s,\theta}^{j} - \frac{1}{R_\theta^j} v_{0j} \cdot sin\beta - \varphi_\theta^j \cdot sin\beta \end{bmatrix} \quad , \quad \begin{bmatrix} \gamma_{0sz}^{j} \\ \gamma_{0\theta z}^{j} \\ \gamma_{1\theta z}^{j} \\ \gamma_{2\theta z}^{j} \end{bmatrix} = \begin{bmatrix} \varphi_s^j + w_{j,s} \\ w_{j,\theta} - v_{0j} \cdot cos\beta \\ -\frac{1}{R_\theta^j} v_{0j} \cdot cos\beta - \varphi_\theta^j \cdot cos\beta \\ \frac{1}{R_\theta^j} v_{0j} + \varphi_\theta^j \end{bmatrix} \tag{11}$$

Initial hoop stress due to centrifugal force with constant angular velocity Ω is defined as (Hua et al., 2005):

$$\sigma_{\theta\theta\_h} = \rho\left|\mathbf{\Omega}\right|^2 r^2 \tag{12}$$

Thus, the stress resultants and moment resultant due to centrifugal force are as follows:

$$\begin{Bmatrix} \bar{N}^j_{\theta\theta} \\ \bar{M}^j_{\theta\theta} \end{Bmatrix} = \int_{-\frac{h_j}{2}}^{\frac{h_j}{2}} \sigma^j_{\theta\theta\_h} \begin{Bmatrix} 1 \\ z_j \end{Bmatrix} dz_j = \int_{-\frac{h_j}{2}}^{\frac{h_j}{2}} (\rho_j \cdot \Omega^2 \cdot (s \cdot \sin\beta + (z_j \pm \frac{h_c + h_j}{2}) \cdot cos\beta)^2) \begin{Bmatrix} 1 \\ z_j \end{Bmatrix} dz_j \tag{13}$$

where plus and minus signs are for the outer and inner face sheet, respectively.

The stress resultants of the core are defined as:

$$\begin{aligned}
\left\{N^c_{zz}, M^c_{z1}, M^c_{z2}, M^c_{z3}\right\} &= \int_{-\frac{h_c}{2}}^{\frac{h_c}{2}} \sigma^c_{zz}(1, z_c, {z_c}^2, {z_c}^3)\, dz_c \\
\left\{Q^c_{sz}, M^c_{Q1sz}, M^c_{Q2sz}, M^c_{Q3sz}\right\} &= \int_{-\frac{h_c}{2}}^{\frac{h_c}{2}} \tau^c_{sz}(1, z_c, {z_c}^2, {z_c}^3)(1 + \frac{z_c}{R^c_\theta})\, dz_c \\
\left\{Q^c_{\theta z}, M^c_{Q1\theta z}, M^c_{Q2\theta z}, M^c_{Q3\theta z}\right\} &= \int_{-\frac{h_c}{2}}^{\frac{h_c}{2}} \tau^c_{\theta z}(1, z_c, {z_c}^2, {z_c}^3) dz_c \\
\left\{N^c_{ss}, M^c_{s1}, M^c_{s2}, M^c_{s3}\right\} &= \int_{-\frac{h_c}{2}}^{\frac{h_c}{2}} \sigma^c_{ss}(1, z_c, {z_c}^2, {z_c}^3)(1 + \frac{z_c}{R^c_\theta}) dz_c \\
\left\{Q^c_{s\theta}, M^c_{Q1s\theta}, M^c_{Q2s\theta}, M^c_{Q3s\theta}\right\} &= \int_{-\frac{h_c}{2}}^{\frac{h_c}{2}} \tau^c_{s\theta}(1, z_c, {z_c}^2, {z_c}^3)(1 + \frac{z_c}{R^c_\theta}) dz_c \\
\left\{Q^c_{\theta s}, M^c_{Q1\theta s}, M^c_{Q2\theta s}, M^c_{Q3\theta s}\right\} &= \int_{-\frac{h_c}{2}}^{\frac{h_c}{2}} \tau^c_{\theta s}(1, z_c, {z_c}^2, {z_c}^3) dz_c \\
\left\{N^c_{\theta\theta}, M^c_{\theta 1}, M^c_{\theta 2}, M^c_{\theta 3}\right\} &= \int_{-\frac{h_c}{2}}^{\frac{h_c}{2}} \sigma^c_{\theta\theta}(1, z_c, {z_c}^2, {z_c}^3) dz_c
\end{aligned} \tag{14}$$

$$\left\{\overline{N}^{c}_{\theta\theta}, \overline{M}^{c}_{\theta 1}, \overline{M}^{c}_{\theta 2}, \overline{M}^{c}_{\theta 3}\right\} = \int_{-\frac{h_c}{2}}^{\frac{h_c}{2}} \sigma^{c}_{\theta\theta\_h}(1, z_c, {z_c}^2, {z_c}^3) dz_c$$

where $\sigma^{c}_{\theta\theta\_h}$ is the initial hoop stress due to centrifugal force.

3.5 Governing Equations

The governing equations are derived through the Hamilton principle. Statement of the Hamilton's principle reads:

$$\int_{t_1}^{t_2} \delta L dt = \int_{t}^{t_2} \delta[T - (U + V)] dt = 0 \tag{15}$$

where T, U and V are the kinetic energy, strain energy and potential of external works of the shell, respectively. Also, t is the time coordinate between the times t_1 and t_2, and δ denotes the variational operator.

Potential energy due to external works of the shell is absent for the free vibration problem. Position, velocity and acceleration vectors of a rotating sandwich conical shell element are assigned as follows:

$$\begin{aligned} \mathbf{r} &= u\vec{\mathbf{i}} + v\vec{\mathbf{j}} + w\vec{\mathbf{k}} \\ \mathbf{v} &= \dot{\mathbf{r}} + \boldsymbol{\Omega} \times \mathbf{r} \\ \mathbf{a} &= \dot{\boldsymbol{\Omega}} \times \mathbf{r} + \boldsymbol{\Omega} \times (\boldsymbol{\Omega} \times \mathbf{r}) + 2\boldsymbol{\Omega} \times \mathbf{v} \end{aligned} \tag{16}$$

where in acceleration statement, second and third parts exist due to centrifugal and Coriolis effects, and $\vec{\mathbf{i}}$, $\vec{\mathbf{j}}$ and $\vec{\mathbf{k}}$ are the unit vectors in s, ϑ and z directions, respectively. Also, Ω is the angular velocity of rotation:

$$\boldsymbol{\Omega} = (-\Omega\cos\beta)\vec{\mathbf{i}} + (\Omega\sin\beta)\vec{\mathbf{k}} \tag{17}$$

So, the first variation of the kinetic energy for the rotating sandwich shell reads:

$$\delta T = \sum_{j=o,c,i} \int_{V_j} \rho_j \left(\dot{u}_j\, \delta\dot{u}_j + \dot{v}_j\, \delta\dot{v}_j + \dot{w}_j\, \delta\dot{w}_j \right) dV_j \tag{18}$$

Here, symbol $(\dot{})$ shows the derivative with respect to time t. Besides δU is the virtual strain energy of the panel, which can be derived as:

$$\begin{aligned}\delta U = &\sum_{j=o,i,c}\int_{V_j}\left(\sigma_{ss}^{j}\,\delta\varepsilon_{ss}^{j}+\sigma_{\theta\theta}^{j}\,\delta\varepsilon_{\theta\theta}^{j}+\sigma_{zz}^{j}\,\delta\varepsilon_{zz}^{j}+\tau_{s\theta}^{j}\,\delta\gamma_{s\theta}^{j}+\tau_{sz}^{j}\,\delta\gamma_{sz}^{j}+\tau_{\theta z}^{j}\,\delta\gamma_{\theta z}^{j}\right)dV_j\\ &+\delta\int_0^L\int_0^{2\pi}\{(R_\theta^o-\frac{h_o}{2})[\lambda_{so}(u_o(z_o=-h_o/2)-u_c(z_c=h_c/2))\\ &+\lambda_{\theta o}(v_o(z_o=-h_o/2)-v_c(z_c=h_c/2))+\lambda_{zo}(w_o-w_c(z_c=h_c/2))]\\ &+(R_\theta^i+\frac{h_i}{2})[\lambda_{si}(u_c(z_c=-h_c/2)-u_i(z_i=h_i/2))\\ &+\lambda_{\theta i}(v_c(z_c=-h_c/2)-v_i(z_i=h_i/2))+\lambda_{zi}(w_c(z_c=-h_c/2)-w_i)]\}d\theta ds\end{aligned}\tag{19}$$

where σ_{ss}^{j} and $\sigma_{\vartheta\vartheta}^{j}$ (j = c, o, i) are the in-plane normal stresses and ε_{ss}^{j} and $\varepsilon_{\vartheta\vartheta}^{j}$ ($j = c, o, i$) are the in-plane normal strains of the core, outer and inner face sheets, respectively; $\tau_{s\vartheta}^{j}$ and $\gamma_{s\vartheta}^{j}$ ($j = c, o, i$) are the in-plane shear stresses and strains in the core and face sheets; σ_{zz}^{j} and ε_{zz}^{j} are the normal stresses and normal strains in the vertical direction of the core; τ_{sz}^{j}, $\tau_{\vartheta z}^{j}$, γ_{sz}^{j} and $\gamma_{\vartheta z}^{j}$ are the vertical shear stresses and vertical shear strains; V_j ($j = c, o, i$) are the volume of the core, outer and inner face sheets, respectively; and λ_{sj}, $\lambda_{\vartheta j}$ and λ_{zj} ($j = o, i$) are the six Lagrange multipliers or compatibility conditions at the outer and inner face sheet-core interfaces.

Because of the centrifugal force of rotation, initial hoop tension produces. This must be noticed in potential energy:

$$\delta U_h = \sum_{j=o,i,c}\int_{V_j}\sigma_{\theta\theta\_h}^{j}\delta\varepsilon_{\theta\theta}^{j}\,dV_j\tag{20}$$

To see the effects of initial mechanical stresses in the equations of motion, the nonlinear terms in the strain relations should be noticed (Malekzadeh and Heydarpour, 2013). By applying the resultant forces and moments and using integration by part technique, as well as using Eqs. (15)– (20), and after some algebraic manipulation, the equations of equilibrium are calculated:
Five equations for the outer face sheet:

$$\begin{aligned}&R_\theta^o N_{ss,s}^o+(N_{ss}^o-N_{\theta\theta}^o-\bar{N}_{\theta\theta}^o)\tan\beta+\frac{1}{\cos\beta}N_{\theta s,\theta}^o-(R_\theta^o-\frac{h_o}{2})\lambda_{so}=\\ &\quad \mathrm{I}_0^o(-\Omega^2\sin^2\beta u_{0o}-\Omega^2\sin\beta\cos\beta w_{0o}+\ddot{u}_{0o}-2\Omega\sin\beta\dot{v}_{0o})\\ &\quad +\mathrm{I}_1^o(-\Omega^2\sin^2\beta\varphi_s^o+\ddot{\varphi}_s^o-2\Omega\sin\beta(\frac{1}{R_\theta^o}\dot{v}_{0o}+\dot{\varphi}_\theta^o))\\ &R_\theta^o M_{ss,s}^o+(M_{ss}^o-M_{\theta\theta}^o-\bar{M}_{\theta\theta}^o)\tan\beta+\frac{1}{\cos\beta}M_{\theta s,\theta}^o-R_\theta^o Q_{sz}^o+(R_\theta^o-\frac{h_o}{2})\frac{h_o}{2}\lambda_{so}=\\ &\quad \mathrm{I}_1^o(-\Omega^2\sin^2\beta u_{0o}-\Omega^2\sin\beta\cos\beta w_{0o}+\ddot{u}_{0o}-2\Omega\sin\beta\dot{v}_{0o})+\mathrm{I}_2^o(-\Omega^2\sin^2\beta\varphi_s^o+\ddot{\varphi}_s^o)\\ &\frac{1}{\cos\beta}N_{\theta\theta,\theta}^o+\frac{1}{B^o}M_{\theta\theta,\theta}^o+\tan\beta(N_{s\theta}^o+N_{\theta s}^o)+R_\theta^o N_{s\theta,s}^o+M_{s\theta,s}^o+\frac{\tan\beta}{R_\theta^o}M_{\theta s}^o\\ &\quad -(R_\theta^o-\frac{h_o}{2})(1-\frac{h_o}{2R_\theta^o})\lambda_{\theta o}=\mathrm{I}_0^o(-\Omega^2 v_{0o}+\ddot{v}_{0o}+2\Omega\cos\beta\dot{w}_{0o}+2\Omega\sin\beta\dot{u}_{0o})\\ &\quad +\mathrm{I}_1^o(-\Omega^2(\frac{1}{R_\theta^o}v_{0o}+\varphi_\theta^o)+(\frac{1}{R_\theta^o}\ddot{v}_{0o}+\ddot{\varphi}_\theta^o)+2\Omega\sin\beta\dot{\varphi}_s^o-\Omega^2 v_{0o}\frac{1}{R_\theta^o}+\ddot{v}_{0o}\frac{1}{R_\theta^o}\\ &\quad +2\Omega\cos\beta\dot{w}_{0o}\frac{1}{R_\theta^o}+2\Omega\sin\beta\dot{u}_{0o}\frac{1}{R_\theta^o})+\mathrm{I}_2^o(-\Omega^2(\frac{1}{R_\theta^o}v_{0o}+\varphi_\theta^o)\frac{1}{R_\theta^o}+(\frac{1}{R_\theta^o}\ddot{v}_{0o}+\ddot{\varphi}_\theta^o)\frac{1}{R_\theta^o}+2\Omega\sin\beta\dot{\varphi}_s^o\frac{1}{R_\theta^o})\\ &\frac{1}{\cos\beta}M_{\theta\theta,\theta}^o+(M_{s\theta}^o+M_{\theta s}^o)\tan\beta+R_\theta^o M_{s\theta,s}^o-R_\theta^o Q_{\theta z}^o+(R_\theta^o-\frac{h_o}{2})\frac{h_o}{2}\lambda_{\theta o}=\\ &\quad \mathrm{I}_1^o(-\Omega^2 v_{0o}+\ddot{v}_{0o}+2\Omega\cos\beta\dot{w}_{0o}+2\Omega\sin\beta\dot{u}_{0o})+\mathrm{I}_2^o(-2\Omega\sin\beta\dot{\varphi}_\theta^o-\Omega^2\varphi_\theta^o\end{aligned}\tag{21}$$

$$
\begin{aligned}
&+\ddot{\varphi}_{\theta}^{o}+2\Omega\sin\beta\dot{\varphi}_{s}^{o}-\Omega^{2}(\frac{1}{R_{\theta}^{o}}v_{0o}+\varphi_{\theta}^{o})+(\frac{1}{R_{\theta}^{o}}\ddot{v}_{0o}+\ddot{\varphi}_{\theta}^{o})+2\Omega\sin\beta\dot{\varphi}_{s}^{o})\\
-(N_{\theta\theta}^{o}+\bar{N}_{\theta\theta}^{o})&+\frac{C2(\bar{N}_{\theta\theta}^{o})}{B^{o}\cos\beta}w_{o,\theta\theta}-\frac{C2(\bar{M}_{\theta\theta}^{o})}{B^{o2}}w_{o,\theta\theta}+\tan\beta Q_{sz}^{o}+R_{\theta}^{o}Q_{sz,s}^{o}\\
&+\frac{1}{\cos\beta}Q_{\theta z,\theta}^{o}-(R_{\theta}^{o}-\frac{h_{o}}{2})\lambda_{zo}=\mathrm{I}_{0}^{o}(-\Omega^{2}\sin\beta\cos\beta u_{0o}-\Omega^{2}\cos^{2}\beta w_{0o}+\ddot{w}_{0o}-2\Omega\cos\beta\dot{v}_{0o})\\
&+\mathrm{I}_{1}^{o}(-\Omega^{2}\sin\beta\cos\beta\varphi_{s}^{o}-2\Omega\cos\beta\dot{\varphi}_{\theta}^{o}-2\Omega\cos\beta\frac{1}{R_{\theta}^{o}}\dot{v}_{0o})
\end{aligned}
$$

Five equations for the inner face sheet:

$$
\begin{aligned}
&R_{\theta}^{i}N_{ss,s}^{i}+(N_{ss}^{i}-N_{\theta\theta}^{i}-\bar{N}_{\theta\theta}^{i})\tan\beta+\frac{1}{\cos\beta}N_{\theta s,\theta}^{i}+(R_{\theta}^{i}+\frac{h_{i}}{2})\lambda_{si}=\\
&\quad\mathrm{I}_{0}^{i}(-\Omega^{2}\sin^{2}\beta u_{0i}-\Omega^{2}\sin\beta\cos\beta w_{0i}+\ddot{u}_{0i}-2\Omega\sin\beta\dot{v}_{0i})\\
&\quad+\mathrm{I}_{1}^{i}(-\Omega^{2}\sin^{2}\beta\varphi_{s}^{i}+\ddot{\varphi}_{s}^{i}-2\Omega\sin\beta(\frac{1}{R_{\theta}^{i}}\dot{v}_{0i}+\dot{\varphi}_{\theta}^{i}))\\
&R_{\theta}^{i}M_{ss,s}^{i}+(M_{ss}^{i}-M_{\theta\theta}^{i}-\bar{M}_{\theta\theta}^{i})\tan\beta+\frac{1}{\cos\beta}M_{\theta s,\theta}^{i}-R_{\theta}^{i}Q_{sz}^{i}+(R_{\theta}^{i}+\frac{h_{i}}{2})\frac{h_{i}}{2}\lambda_{si}=\\
&\quad\mathrm{I}_{1}^{i}(-\Omega^{2}\sin^{2}\beta u_{0i}-\Omega^{2}\sin\beta\cos\beta w_{0i}+\ddot{u}_{0i}-2\Omega\sin\beta\dot{v}_{0i})+\mathrm{I}_{2}^{o}(-\Omega^{2}\sin^{2}\beta\varphi_{s}^{i}+\ddot{\varphi}_{s}^{i})\\
&\frac{1}{\cos\beta}N_{\theta\theta,\theta}^{i}+\frac{1}{B^{i}}M_{\theta\theta,\theta}^{i}+\tan\beta(N_{s\theta}^{i}+N_{\theta s}^{i})+R_{\theta}^{i}N_{s\theta,s}^{i}+M_{s\theta,s}^{i}+\frac{\tan\beta}{R_{\theta}^{i}}M_{\theta s}^{i}\\
&\quad+(R_{\theta}^{i}+\frac{h_{i}}{2})(1+\frac{h_{i}}{2R_{\theta}^{i}})\lambda_{\theta i}=\mathrm{I}_{0}^{i}(-\Omega^{2}v_{0i}+\ddot{v}_{0i}+2\Omega\cos\beta\dot{w}_{0i}+2\Omega\sin\beta\dot{u}_{0i})\\
&\quad+\mathrm{I}_{1}^{i}(-\Omega^{2}(\frac{1}{R_{\theta}^{i}}v_{0i}+\varphi_{\theta}^{i})+(\frac{1}{R_{\theta}^{i}}\ddot{v}_{0i}+\ddot{\varphi}_{\theta}^{i})+2\Omega\sin\beta\dot{\varphi}_{s}^{i}-\Omega^{2}v_{0i}\frac{1}{R_{\theta}^{i}}+\ddot{v}_{0i}\frac{1}{R_{\theta}^{i}}+2\Omega\cos\beta\dot{w}_{0i}\frac{1}{R_{\theta}^{i}}+2\Omega\sin\beta\dot{u}_{0i}\frac{1}{R_{\theta}^{i}})\\
&\quad+\mathrm{I}_{2}^{i}(-\Omega^{2}(\frac{1}{R_{\theta}^{i}}v_{0i}+\varphi_{\theta}^{i})\frac{1}{R_{\theta}^{i}}+(\frac{1}{R_{\theta}^{i}}\ddot{v}_{0i}+\ddot{\varphi}_{\theta}^{i})\frac{1}{R_{\theta}^{i}}+2\Omega\sin\beta\dot{\varphi}_{s}^{i}\frac{1}{R_{\theta}^{i}})\\
&\frac{1}{\cos\beta}M_{\theta\theta,\theta}^{i}+(M_{s\theta}^{i}+M_{\theta s}^{i})\tan\beta+R_{\theta}^{i}M_{s\theta,s}^{i}-R_{\theta}^{i}Q_{\theta z}^{i}+(R_{\theta}^{i}+\frac{h_{i}}{2})\frac{h_{i}}{2}\lambda_{\theta i}=\\
&\quad\mathrm{I}_{1}^{i}(-\Omega^{2}v_{0i}+\ddot{v}_{0i}+2\Omega\cos\beta\dot{w}_{0i}+2\Omega\sin\beta\dot{u}_{0i})+\mathrm{I}_{2}^{i}(-2\Omega\sin\beta\dot{\varphi}_{\theta}^{i}-\Omega^{2}\varphi_{\theta}^{i}\\
&\quad+\ddot{\varphi}_{\theta}^{i}+2\Omega\sin\beta\dot{\varphi}_{s}^{i}-\Omega^{2}(\frac{1}{R_{\theta}^{i}}v_{0i}+\varphi_{\theta}^{i})+(\frac{1}{R_{\theta}^{i}}\ddot{v}_{0i}+\ddot{\varphi}_{\theta}^{i})+2\Omega\sin\beta\dot{\varphi}_{s}^{i})\\
-(N_{\theta\theta}^{i}+\bar{N}_{\theta\theta}^{i})&+\frac{C2(\bar{N}_{\theta\theta}^{i})}{B^{i}\cos\beta}w_{i,\theta\theta}-\frac{C2(\bar{M}_{\theta\theta}^{i})}{B^{i2}}w_{\mathrm{i},\theta\theta}+\tan\beta Q_{sz}^{i}+R_{\theta}^{i}Q_{sz,s}^{i}\\
&+\frac{1}{\cos\beta}Q_{\theta z,\theta}^{i}+(R_{\theta}^{i}+\frac{h_{i}}{2})\lambda_{zi}=\mathrm{I}_{0}^{i}(-\Omega^{2}\sin\beta\cos\beta u_{0i}-\Omega^{2}\cos^{2}\beta w_{0i}+\ddot{w}_{0i}-2\Omega\cos\beta\dot{v}_{0i})\\
&+\mathrm{I}_{1}^{i}(-\Omega^{2}\sin\beta\cos\beta\varphi_{s}^{i}-2\Omega\cos\beta\dot{\varphi}_{\theta}^{i}-2\Omega\cos\beta\frac{1}{R_{\theta}^{i}}\dot{v}_{0i})
\end{aligned}
\tag{22}
$$

Eleven equations for the core:

$$
\begin{aligned}
&R_{\theta}^{c}N_{ss,s}^{c}+(N_{ss}^{c}-N_{\theta}^{c}-\bar{N}_{\theta}^{c})\tan\beta+\frac{1}{\cos\beta}Q_{\theta s,\theta}^{c}+(R_{\theta}^{o}-\frac{h_{o}}{2})\lambda_{so}-(R_{\theta}^{i}+\frac{h_{i}}{2})\lambda_{si}=\\
&\quad I_{0}^{c}(-\Omega^{2}\sin^{2}\beta u_{0c}-\Omega^{2}\sin\beta\cos\beta w_{0c}+\ddot{u}_{0c}-2\Omega\sin\beta\dot{v}_{0c})\\
&\quad+I_{1}^{c}(-\Omega^{2}\sin^{2}\beta u_{1c}-\Omega^{2}\sin\beta\cos\beta w_{1c}+\ddot{u}_{1c}-2\Omega\sin\beta(1\ /\ R_{\theta}^{c})\dot{v}_{0c}-2\Omega\sin\beta\dot{v}_{1c})\\
&\quad+I_{2}^{c}(-\Omega^{2}\sin^{2}\beta u_{2c}-\Omega^{2}\sin\beta\cos\beta w_{2c}+\ddot{u}_{2c}-2\Omega\sin\beta\dot{v}_{2c})\\
&\quad+I_{3}^{c}(-\Omega^{2}\sin^{2}\beta u_{3c}+\ddot{u}_{3c}-2\Omega\sin\beta\dot{v}_{3c})
\end{aligned}
\tag{23}
$$

$$R_\theta^c M_{s1,s}^c + (M_{s1}^c - M_{\theta1}^c - \bar{M}_{\theta1}^c)\tan\beta + \frac{1}{\cos\beta}\mathrm{M}_{Q1\theta s,\theta}^c - R_\theta^c Q_{sz}^c + (R_\theta^o - \frac{h_o}{2})\frac{h_c}{2}\lambda_{so} + (R_\theta^i + \frac{h_i}{2})\frac{h_c}{2}\lambda_{si} =$$
$$I_1^c(-\Omega^2\sin^2\beta u_{0c} - \Omega^2\sin\beta\cos\beta w_{0c} + \ddot{u}_{0c} - 2\Omega\sin\beta\dot{v}_{0c})$$
$$+I_2^c(-\Omega^2\sin^2\beta u_{1c} - \Omega^2\sin\beta\cos\beta w_{1c} + \ddot{u}_{1c} - 2\Omega\sin\beta(1\ /\ R_\theta^c)\dot{v}_{0c} - 2\Omega\sin\beta\dot{v}_{1c})$$
$$+I_3^c(-\Omega^2\sin^2\beta u_{2c} - \Omega^2\sin\beta\cos\beta w_{2c} + \ddot{u}_{2c} - 2\Omega\sin\beta\dot{v}_{2c})$$
$$+I_4^c(-\Omega^2\sin^2\beta u_{3c} + \ddot{u}_{3c} - 2\Omega\sin\beta\dot{v}_{3c})$$

$$R_\theta^c M_{s2,s}^c + (M_{s2}^c - M_{\theta2}^c - \bar{M}_{\theta2}^c)\tan\beta + \frac{1}{\cos\beta}\mathrm{M}_{Q2\theta s,\theta}^c - 2R_\theta^c M_{Q1sz}^c + (R_\theta^o - \frac{h_o}{2})\frac{{h_c}^2}{4}\lambda_{so} - (R_\theta^i + \frac{h_i}{2})\frac{{h_c}^2}{4}\lambda_{si} =$$
$$I_2^c(-\Omega^2\sin^2\beta u_{0c} - \Omega^2\sin\beta\cos\beta w_{0c} + \ddot{u}_{0c} - 2\Omega\sin\beta\dot{v}_{0c})$$
$$+I_3^c(-\Omega^2\sin^2\beta u_{1c} - \Omega^2\sin\beta\cos\beta w_{1c} + \ddot{u}_{1c} - 2\Omega\sin\beta(1\ /\ R_\theta^c)\dot{v}_{0c} - 2\Omega\sin\beta\dot{v}_{1c})$$
$$+I_4^c(-\Omega^2\sin^2\beta u_{2c} - \Omega^2\sin\beta\cos\beta w_{2c} + \ddot{u}_{2c} - 2\Omega\sin\beta\dot{v}_{2c})$$
$$+I_5^c(-\Omega^2\sin^2\beta u_{3c} + \ddot{u}_{3c} - 2\Omega\sin\beta\dot{v}_{3c})$$

$$R_\theta^c M_{s3,s}^c + (M_{s3}^c - M_{\theta3}^c - \bar{M}_{\theta3}^c)\tan\beta + \frac{1}{\cos\beta}\mathrm{M}_{Q3\theta s,\theta}^c - 3R_\theta^c M_{Q2sz}^c + (R_\theta^o - \frac{h_o}{2})\frac{{h_c}^3}{8}\lambda_{so} + (R_\theta^i + \frac{h_i}{2})\frac{{h_c}^3}{8}\lambda_{si} =$$
$$I_3^c(-\Omega^2\sin^2\beta u_{0c} - \Omega^2\sin\beta\cos\beta w_{0c} + \ddot{u}_{0c} - 2\Omega\sin\beta\dot{v}_{0c})$$
$$+I_4^c(-\Omega^2\sin^2\beta u_{1c} - \Omega^2\sin\beta\cos\beta w_{1c} + \ddot{u}_{1c} - 2\Omega\sin\beta(1\ /\ R_\theta^c)\dot{v}_{0c} - 2\Omega\sin\beta\dot{v}_{1c})$$
$$+I_5^c(-\Omega^2\sin^2\beta u_{2c} - \Omega^2\sin\beta\cos\beta w_{2c} + \ddot{u}_{2c} - 2\Omega\sin\beta\dot{v}_{2c})$$
$$+I_6^c(-\Omega^2\sin^2\beta u_{3c} + \ddot{u}_{3c} - 2\Omega\sin\beta\dot{v}_{3c})$$

$$\frac{1}{\cos\beta}N_{\theta\theta,\theta}^c + \frac{1}{B^c}M_{\theta1,\theta}^c + R_\theta^c Q_{s\theta,s}^c + \frac{\tan\beta}{R_\theta^c}(\mathrm{M}_{Q1s\theta}^c + \mathrm{M}_{Q1\theta s}^c) + \mathrm{M}_{Q1s\theta,s}^c + \tan\beta(Q_{s\theta}^c + Q_{\theta s}^c) + (R_\theta^o - \frac{h_o}{2})(1 + \frac{h_c}{2R_\theta^c})\lambda_{\theta o}$$
$$-(R_\theta^i + \frac{h_i}{2})(1 - \frac{h_c}{2R_\theta^c})\lambda_{\theta i} = I_0^c(-\Omega^2 v_{0c} + \ddot{v}_{0c} + 2\Omega\cos\beta\dot{w}_{0c} + 2\Omega\sin\beta\dot{u}_{0c})$$
$$+I_1^c(-\Omega^2(1\ /\ R_\theta^c)v_{0c} - \Omega^2 v_{1c} + (1\ /\ R_\theta^c)\ddot{v}_{0c} + \ddot{v}_{1c} + 2\Omega\cos\beta\dot{w}_{1c} + 2\Omega\sin\beta\dot{u}_{1c}$$
$$-\Omega^2 v_{0c}(1\ /\ R_\theta^c) + \ddot{v}_{0c}(1\ /\ R_\theta^c) + 2\Omega\cos\beta\dot{w}_{0c}(1\ /\ R_\theta^c) + 2\Omega\sin\beta\dot{u}_{0c}(1\ /\ R_\theta^c))$$
$$+I_2^c(-\Omega^2 v_{2c} + \ddot{v}_{2c} + 2\Omega\cos\beta\dot{w}_{2c} + 2\Omega\sin\beta\dot{u}_{2c} - \Omega^2(1\ /\ R_\theta^c)^2 v_{0c} - \Omega^2 v_{1c}(1\ /\ R_\theta^c)$$
$$+(1\ /\ R_\theta^c)^2\ddot{v}_{0c} + \ddot{v}_{1c}(1\ /\ R_\theta^c) + 2\Omega\cos\beta\dot{w}_{1c}(1\ /\ R_\theta^c) + 2\Omega\sin\beta\dot{u}_{1c}(1\ /\ R_\theta^c))$$
$$+I_3^c(-\Omega^2 v_{3c} + \ddot{v}_{3c} + 2\Omega\sin\beta\dot{u}_{3c} - \Omega^2 v_{2c}(1\ /\ R_\theta^c) + \ddot{v}_{2c}(1\ /\ R_\theta^c)$$
$$+2\Omega\cos\beta\dot{w}_{2c}(1\ /\ R_\theta^c) + 2\Omega\sin\beta\dot{u}_{2c}(1\ /\ R_\theta^c))$$
$$+I_4^c(-\Omega^2 v_{3c}(1\ /\ R_\theta^c) + \ddot{v}_{3c}(1\ /\ R_\theta^c) + 2\Omega\sin\beta\dot{u}_{3c}(1\ /\ R_\theta^c))$$

$$\frac{1}{\cos\beta}M_{\theta1,\theta}^c + R_\theta^c\,\mathrm{M}_{Q1s\theta,s}^c + \tan\beta(\mathrm{M}_{Q1s\theta}^c + \mathrm{M}_{Q1\theta s}^c) - R_\theta^c Q_{\theta z}^c + (R_\theta^o - \frac{h_o}{2})\frac{h_c}{2}\lambda_{\theta o} + (R_\theta^i + \frac{h_i}{2})\frac{h_c}{2}\lambda_{\theta i} =$$
$$I_1^c(-\Omega^2 v_{0c} + \ddot{v}_{0c} + 2\Omega\cos\beta\dot{w}_{0c} + 2\Omega\sin\beta\dot{u}_{0c})$$
$$+I_2^c(-\Omega^2(1\ /\ R_\theta^c)v_{0c} - \Omega^2 v_{1c} + (1\ /\ R_\theta^c)\ddot{v}_{0c} + \ddot{v}_{1c} + 2\Omega\cos\beta\dot{w}_{1c} + 2\Omega\sin\beta\dot{u}_{1c})$$
$$+I_3^c(-\Omega^2 v_{2c} + \ddot{v}_{2c} + 2\Omega\cos\beta\dot{w}_{2c} + 2\Omega\sin\beta\dot{u}_{2c})$$
$$+I_4^c(-\Omega^2 v_{3c} + \ddot{v}_{3c} + 2\Omega\sin\beta\dot{u}_{3c})$$

$$\frac{1}{\cos\beta}M_{\theta2,\theta}^c + R_\theta^c\,\mathrm{M}_{Q2s\theta,s}^c + \tan\beta(\mathrm{M}_{Q2s\theta}^c + \mathrm{M}_{Q2\theta s}^c) - 2R_\theta^c M_{Q1\theta z}^c - M_{Q2\theta z}^c + (R_\theta^o - \frac{h_o}{2})\frac{{h_c}^2}{4}\lambda_{\theta o}$$
$$-(R_\theta^i + \frac{h_i}{2})\frac{{h_c}^2}{4}\lambda_{\theta i} = I_2^c(-\Omega^2 v_{0c} + \ddot{v}_{0c} + 2\Omega\cos\beta\dot{w}_{0c} + 2\Omega\sin\beta\dot{u}_{0c})$$

$$
\begin{aligned}
&+I_3^c(-\Omega^2(1\ /\ R_\theta^c)v_{0c} - \Omega^2 v_{1c} + (1\ /\ R_\theta^c)\ddot{v}_{0c} + 2\Omega\cos\beta\dot{w}_{1c} + 2\Omega\sin\beta\dot{u}_{1c})\\
&+I_4^c(-\Omega^2 v_{2c} + \ddot{v}_{2c} + 2\Omega\cos\beta\dot{w}_{2c} + 2\Omega\sin\beta\dot{u}_{2c})\\
&+I_5^c(-\Omega^2 v_{3c} + \ddot{v}_{3c} + 2\Omega\sin\beta\dot{u}_{3c})
\end{aligned}
$$

$$
\begin{aligned}
&\frac{1}{\cos\beta}M_{\theta 3,\theta}^c + R_\theta^c\,\mathrm{M}_{Q3s\theta,s}^c + (\mathrm{M}_{Q3s\theta}^c + \mathrm{M}_{Q3\theta s}^c)\tan\beta - 3R_\theta^c M_{Q2\theta z}^c - 2M_{Q3\theta z}^c + (R_\theta^o - \frac{h_o}{2})\frac{{h_c}^3}{8}\lambda_{\theta o}\\
&\quad +(R_\theta^i + \frac{h_i}{2})\frac{{h_c}^3}{8}\lambda_{\theta i} = I_3^c(-\Omega^2 v_{0c} + \ddot{v}_{0c} + 2\Omega\cos\beta\dot{w}_{0c} + 2\Omega\sin\beta\dot{u}_{0c})\\
&\quad +I_4^c(-\Omega^2(1\ /\ R_\theta^c)v_{0c} - \Omega^2 v_{1c} + (1\ /\ R_\theta^c)\ddot{v}_{0c} + \ddot{v}_{1c} + 2\Omega\cos\beta\dot{w}_{1c} + 2\Omega\sin\beta\dot{u}_{1c})\\
&\quad +I_5^c(-\Omega^2 v_{2c} + \ddot{v}_{2c} + 2\Omega\cos\beta\dot{w}_{2c} + 2\Omega\sin\beta\dot{u}_{2c})\\
&\quad +I_6^c(-\Omega^2 v_{3c} + \ddot{v}_{3c} + 2\Omega\sin\beta\dot{u}_{3c})\\
&-(N_{\theta\theta}^c + \bar{N}_{\theta\theta}^c) + \frac{C2(\bar{N}_{\theta\theta}^c)}{B^c\cos\beta}w_{0,\theta\theta} - \frac{C2(\bar{M}_{\theta 1}^c)}{B^{c2}}w_{0,\theta\theta} + \frac{C2.\cos\beta(\bar{M}_{\theta 2}^c)}{B^{c3}}w_{0,\theta\theta} - \frac{C2.\cos^2\beta(\bar{M}_{\theta 3}^c)}{B^{c4}}w_{0,\theta\theta}\\
&\quad +R_\theta^c Q_{sz,s}^c + \tan\beta Q_{sz}^c + \frac{1}{\cos\beta}Q_{\theta z,\theta}^c + (R_\theta^o - \frac{h_o}{2})\lambda_{zo} - (R_\theta^i + \frac{h_i}{2})\lambda_{zi} =\\
&\quad I_0^c(-\Omega^2\sin\beta\cos\beta u_{0c} - \Omega^2\cos^2\beta w_{0c} + \ddot{w}_{0c} - 2\Omega\cos\beta\dot{v}_{0c})\\
&\quad +I_1^c(-\Omega^2\sin\beta\cos\beta u_{1c} - \Omega^2\cos^2\beta w_{1c} + \ddot{w}_{1c} - 2\Omega\cos\beta(1\ /\ R_\theta^c)\dot{v}_{0c} - 2\Omega\cos\beta\dot{v}_{1c})\\
&\quad +I_2^c(-\Omega^2\sin\beta\cos\beta u_{2c} - \Omega^2\cos^2\beta w_{2c} + \ddot{w}_{2c} - 2\Omega\cos\beta\dot{v}_{2c})\\
&\quad +I_3^c(-\Omega^2\sin\beta\cos\beta u_{3c} - 2\Omega\cos\beta\dot{v}_{3c})\\
&-(M_{\theta 1}^c + \bar{M}_{\theta 1}^c) + R_\theta^c M_{Q1sz,s}^c + \tan\beta M_{Q1sz}^c + \frac{1}{\cos\beta}M_{Q1\theta z,\theta}^c - R_\theta^c N_{zz}^c - M_{z1}^c + (R_\theta^o - \frac{h_o}{2})\frac{h_c}{2}\lambda_{zo}\\
&\quad +(R_\theta^i + \frac{h_i}{2})\frac{h_c}{2}\lambda_{zi} = I_1^c(-\Omega^2\sin\beta\cos\beta u_{0c} - \Omega^2\cos^2\beta w_{0c} + \ddot{w}_{0c} - 2\Omega\cos\beta\dot{v}_{0c})\\
&\quad +I_2^c(-\Omega^2\sin\beta\cos\beta u_{1c} - \Omega^2\cos^2\beta w_{1c} + \ddot{w}_{1c} - 2\Omega\cos\beta(1\ /\ R_\theta^c)\dot{v}_{0c} - 2\Omega\cos\beta\dot{v}_{1c})\\
&\quad +I_3^c\{(-\Omega^2\sin\beta\cos\beta u_{2c} - \Omega^2\cos^2\beta w_{2c} + \ddot{w}_{2c} - 2\Omega\cos\beta\dot{v}_{2c})\\
&\quad +I_4^c(-\Omega^2\sin\beta\cos\beta u_{3c} - 2\Omega\cos\beta\dot{v}_{3c})\\
&-(M_{\theta 2}^c + \bar{M}_{\theta 2}^c) + R_\theta^c M_{Q2sz,s}^c + \tan\beta M_{Q2sz}^c + \frac{1}{\cos\beta}M_{Q2\theta z,\theta}^c - 2R_\theta^c M_{z1}^c - 2M_{z2}^c + (R_\theta^o - \frac{h_o}{2})\frac{{h_c}^2}{4}\lambda_{zo}\\
&\quad -(R_\theta^i + \frac{h_i}{2})\frac{{h_c}^2}{4}\lambda_{zi} = I_2^c(-\Omega^2\sin\beta\cos\beta u_{0c} - \Omega^2\cos^2\beta w_{0c} + \ddot{w}_{0c} - 2\Omega\cos\beta\dot{v}_{0c})\\
&\quad +I_3^c(-\Omega^2\sin\beta\cos\beta u_{1c} - \Omega^2\cos^2\beta w_{1c} + \ddot{w}_{1c} - 2\Omega\cos\beta(1\ /\ R_\theta^c)\dot{v}_{0c} - 2\Omega\cos\beta\dot{v}_{1c})\\
&\quad +I_4^c(-\Omega^2\sin\beta\cos\beta u_{2c} - \Omega^2\cos^2\beta w_{2c} + \ddot{w}_{2c} - 2\Omega\cos\beta\dot{v}_{2c})\\
&\quad +I_5^c(-\Omega^2\sin\beta\cos\beta u_{3c} - 2\Omega\cos\beta\dot{v}_{3c})
\end{aligned}
$$

in which,

$$
I_L^j = \sum_{k=1}^{n}\int_{Z_k}^{Z_{k+1}}\rho_j\cdot z_j^L(R_\theta^j + z_j)dz_j \qquad , \qquad L = 0...6 \tag{24}
$$

Finally, the six compatibility conditions correspond to the perfect bonding at the interface:

$$
\begin{aligned}
&u_{0o} - \frac{h_o}{2}\phi_s^o - u_0 - u_1\frac{h_c}{2} - u_2\frac{{h_c}^2}{4} - u_3\frac{{h_c}^3}{8} = 0\\
&(1 - \frac{h_o}{2R_\theta^o})v_{0o} - \frac{h_o}{2}\phi_\theta^o - (1 + \frac{h_c}{2R_\theta^c})v_0 - v_1\frac{h_c}{2} - v_2\frac{{h_c}^2}{4} - v_3\frac{{h_c}^3}{8} = 0\\
&w_{0o} - w_0 - w_1\frac{h_c}{2} - w_2\frac{{h_c}^2}{4} = 0\\
&u_0 - u_1\frac{h_c}{2} + u_2\frac{{h_c}^2}{4} - u_3\frac{{h_c}^3}{8} - u_{0i} - \frac{h_i}{2}\phi_s^i = 0\\
&(1 - \frac{h_c}{2R_\theta^c})v_0 - v_1\frac{h_c}{2} + v_2\frac{{h_c}^2}{4} - v_3\frac{{h_c}^3}{8} - (1 + \frac{h_i}{2R_\theta^i})v_{0i} - \frac{h_i}{2}\phi_\theta^i = 0\\
&w_0 - w_1\frac{h_c}{2} + w_2\frac{{h_c}^2}{4} - w_{0i} = 0
\end{aligned}
\tag{25}
$$

The governing equations of motion are formulated in terms of the following 27 unknowns: 10 displacements of the mid-plane of the outer and inner face sheets, 6 Lagrange multipliers and 11 polynomial coefficients of the core.

4 ANALYTICAL SOLUTION

In this section, the free vibration of a simply supported rotating sandwich panel is introduced. The present structure consists of laminated composite face sheets that have especially orthotropic construction with laminated composite materials. Furthermore, the core is assumed isotropic. Here, a Galerkin's solution method with 27 trigonometric shape functions is established. A closed form solution is used based on trigonometric functions for a harmonic excitation, which fully satisfy the boundary conditions, including those of the higher-order of the core. Satisfaction of the simply supported boundary conditions at the edges $s = s_1$ and s_2 meets:

$$
\begin{aligned}
&N_{ss}^{\,j} = M_{ss}^{\,j} = v_{0\,j} = \varphi_\theta^{\,j} = w_{\,j} = 0 \qquad\qquad (j = o, i)\\
&N_{ss}^{\,c} = M_{s1}^{\,c} = M_{s2}^{\,c} = M_{s3}^{\,c} = v_0 = v_1 = v_2 = v_3 = w_0 = w_1 = w_2 = 0
\end{aligned}
\tag{26}
$$

So, the solution series reads:

$$
\begin{aligned}
u_{0j}(s,\theta,t) &= (\sum_{n=1}^{N}(\sum_{m=1}^{M} C_{u_{0j}}^{mn}\cos(\frac{m\pi}{L}(s - s_1))\sin(n\theta)))e^{i\omega t}\\
\varphi_s^j(s,\theta,t) &= (\sum_{n=1}^{N}(\sum_{m=1}^{M} C_{\varphi_s^j}^{mn}\cos(\frac{m\pi}{L}(s - s_1))\sin(n\theta)))e^{i\omega t}\\
v_{0j}(s,\theta,t) &= (\sum_{n=1}^{N}(\sum_{m=1}^{M} C_{v_{0j}}^{mn}\sin(\frac{m\pi}{L}(s - s_1))\cos(n\theta)))e^{i\omega t}\\
\varphi_\theta^j(s,\theta,t) &= (\sum_{n=1}^{N}(\sum_{m=1}^{M} C_{\varphi_\theta^j}^{mn}\sin(\frac{m\pi}{L}(s - s_1))\cos(n\theta)))e^{i\omega t}\\
w_j(s,\theta,t) &= (\sum_{n=1}^{N}(\sum_{m=1}^{M} C_{w_j}^{mn}\sin(\frac{m\pi}{L}(s - s_1))\sin(n\theta)))e^{i\omega t}\\
u_k(s,\theta,t) &= (\sum_{n=1}^{N}(\sum_{m=1}^{M} C_{u_k}^{mn}\cos(\frac{m\pi}{L}(s - s_1))\sin(n\theta)))e^{i\omega t} \qquad (k = 0,1,2,3)
\end{aligned}
\tag{27}
$$

$$v_k(s,\theta,t) = (\sum_{n=1}^{N}(\sum_{m=1}^{M} C_{v_k}^{mn} \sin(\frac{m\pi}{L}(s-s_1))\cos(n\theta)))e^{i\omega t} \qquad (k=0,1,2,3)$$

$$w_l(s,\theta,t) = (\sum_{n=1}^{N}(\sum_{m=1}^{M} C_{w_l}^{mn} \sin(\frac{m\pi}{L}(s-s_1))\sin(n\theta)))e^{i\omega t} \qquad (l=0,1,2)$$

$$\lambda_{sj}(s,\theta,t) = (\sum_{n=1}^{N}(\sum_{m=1}^{M} C_{\lambda_{sj}}^{mn} \cos(\frac{m\pi}{L}(s-s_1))\sin(n\theta)))e^{i\omega t}$$

$$\lambda_{\theta j}(s,\theta,t) = (\sum_{n=1}^{N}(\sum_{m=1}^{M} C_{\lambda_{\theta j}}^{mn} \sin(\frac{m\pi}{L}(s-s_1))\cos(n\theta)))e^{i\omega t}$$

$$\lambda_{zj}(s,\theta,t) = (\sum_{n=1}^{N}(\sum_{m=1}^{M} C_{\lambda_{zj}}^{mn} \sin(\frac{m\pi}{L}(s-s_1))\sin(n\theta)))e^{i\omega t}$$

where: C_{kj}^{mn} *(kj=*u_{0o}, v_{0o}, w_o, φ_s^o, φ_ϑ^o, u_{0i}, v_{0i}, w_i, φ_s^i, φ_ϑ^i, $u_{0,1,2,3}$, $v_{0,1,2,3}$, $w_{0,1,2}$, λ_{so}, $\lambda_{\vartheta o}$, λ_{zo}, λ_{si}, $\lambda_{\vartheta i}$, λ_{zi}*)* are the constants of the series solution to be determined.

After substitution of the shape functions into the equilibrium equations, Eqs. (22)– (23), along with the stress resultants of the face sheets and high-order stress resultants of the core, the free vibration equations of motion are transformed into a system of ordinary differential equations as follows:

$$\mathbf{M}\ddot{\mathbf{d}} + \mathbf{C}\dot{\mathbf{d}} + \mathbf{K}\mathbf{d} = \mathbf{0} \tag{28}$$

where $\mathbf{d}$ is the vector of degrees of freedom and ($\dot{}$) and ($\ddot{}$) mean the differentiation of that variable with respect to the variable t. The elements of the mass matrix $\mathbf{M}$, damping matrix $\mathbf{C}$ and stiffness matrix $\mathbf{K}$ are acquired from the discretized form of the equations of motion and related boundary conditions (Malekzadeh and Heydarpour, 2013). It is notable that the effect of Coriolis acceleration is included in the damping matrix $\mathbf{C}$.

Here, since the set of equations is partially algebraic and partially differential, finding of the stiffness matrix is 27, while that of the mass and damping matrices is only 21. However, the corresponding mass, damping and stiffness matrices can be condensed into a dimension of fifteen by removing the following dependent variables (Frostig and Thomsen, 2004):

$$C\lambda_{so},\ C\lambda_{\vartheta o},\ C\lambda_{zo},\ C\lambda_{si},\ C\lambda_{\vartheta i},\ C\lambda_{zi},\ Cu_{2,3},\ Cv_{2,3},\ Cw_{1,2}.$$

Thus, the number of eigenvalues is only 15 for specified values of m and n. 10 out of these 15 eigen frequencies correspond to local modes in the face sheets, and the additional five correspond to local modes in the core. For the sake of brevity, just some nonzero elements of mass, damping and stiffness matrices are presented in Appendix I.

By describing the new degrees of freedom vector $\mathbf{q}$ as:

$$\mathbf{q} = \begin{Bmatrix} \mathbf{d} \\ \dot{\mathbf{d}} \end{Bmatrix} \tag{29}$$

and using state space formulation we rewrite Eq. (28) as:

$$\dot{\mathbf{q}} = \mathbf{A}\mathbf{q} \tag{30}$$

in which:

$$\mathbf{A} = \begin{bmatrix} \mathbf{0} & \mathbf{I} \\ -\mathbf{M}^{-1}\mathbf{K} & -\mathbf{M}^{-1}\mathbf{C} \end{bmatrix} \tag{31}$$

Because Eq. (30) represents a homogeneous set of ODEs, the general solution has the form:

$$\mathbf{q}(t) = \mathbf{Q}\, \mathrm{e}^{\mu t} \tag{32}$$

in which μ is a complex number. By substituting Eq. (32) into Eq. (30) a standard eigenvalue problem can be obtained as:

$$(\mathbf{A} - \mu \mathbf{I})\mathbf{Q} = \mathbf{0} \tag{33}$$

The imaginary parts of the eigenvalues of Eq. (33) are the damped frequencies of the rotating sandwich conical shell.

5 NUMERICAL RESULTS AND DISCUSSION

Here, the accuracy of the presented solution method for the rotating sandwich conical shell is demonstrated by comparing the results with those available in the literature (Hua et al., 2005). Also, the convergence rate of the method is investigated for evaluating the frequencies of the rotating truncated sandwich conical shell. In addition, for more validation, the results of the present formulation have been compared with those programmed in ANSYS. Then, the effects of some parameters such as angular velocity, cone angle, length to radius ratio and core thickness to radius ratio on frequency of rotating sandwich shell have been investigated.

As a first example, since there is no study presented in literature on free vibration analysis of rotating sandwich conical shells with laminated face sheets and isotropic core, the accuracy of the frequency parameters of backward wave for a rotating sandwich conical shell with isotropic face sheets and core is presented. The material properties are shown in Table 1. The results are prepared for the different values of rotating angular velocity (Ω) and five different semi-vertex angles. For the purpose of comparison, the results of the reference by Hua et al. (2005) are also cited.

Layer	E (N/m^2)	v	ϱ (kg/m^3)	Thickness (mm)
Outer	4.8265 x 10^9	0.3	1314	h/5
Core	2.0685 x 10^{11}	0.3	8053	3h/5
Inner	4.8265 x 10^9	0.3	1314	h/5

Table 1: Material property of the sandwich conical shell (Hua et al. (2005)).

The present results and the results given by Hua et al. (2005) has been shown and compared in Table 2. In all cases, the convergence rate is acceptable and very good agreement of the results with those of work by Hua et al. (2005) can be seen. The maximum discrepancy between the results is about 2.54 percent.

Ω	β=5°		β=15°		β=30°		β=45°		β=60°	
	Hua et al. (2005)	Present	Hua et al. (2005)	Present	Hua et al. (2005)	Present	Hua et al. (2005)	Present	Hua et al. (2005)	Present
0	0.0752	0.0735	0.2348	0.2321	0.4202	0.4175	0.4911	0.4887	0.4282	0.4266
2	0.0821	0.0811	0.2493	0.2476	0.4401	0.4392	0.5127	0.5059	0.4471	0.4357
4	0.0889	0.0872	0.2651	0.2587	0.4651	0.4644	0.5423	0.5411	0.4805	0.4796
6	0.1003	0.0981	0.2825	0.2832	0.4952	0.4839	0.5793	0.5681	0.5311	0.5332
8	0.1111	0.1115	0.3063	0.3051	0.5303	0.5321	0.6252	0.6268	0.5923	0.5829
10	0.1238	0.1245	0.3275	0.3263	0.5707	0.5623	0.6754	0.6730	0.6581	0.6524
12	0.1365	0.1345	0.3571	0.3554	0.6108	0.6093	0.7317	0.7321	0.7317	0.7176
14	0.1508	0.1501	0.3809	0.3802	0.6511	0.6447	0.7952	0.7941	0.8112	0.8109
16	0.1651	0.1626	0.4048	0.4033	0.7112	0.7106	0.8525	0.8507	0.8774	0.8754

Table 2: Comparison of frequency parameter ($\boldsymbol{f = \omega r_2\sqrt{\rho_c(1-\upsilon_c^2)/E_c}}$) of backward wave for the rotating sandwich conical shell with simply supported- simply supported boundary condition (m=1, n=2, h/r_1=0.008, L/r_1=20).

In addition, the convergence study of the frequencies of backward wave for the rotating truncated conical sandwich shells with simply supported boundary conditions and material properties according to Table 3 is shown in Table 4. The results are presented for the two different values of semi-vertex angle (β) and angular velocity ($\boldsymbol{\Omega}$). The numerical stability and convergence rate of the present approach show its computational efficiency and promise the correctness of formulation. One also sees that about five circumferential wave numbers are sufficient to obtain the results convergence. Hence, hereafter, five circumferential wave numbers are used to obtain the numerical results.

Layer	Materials	Thickness (mm)	Elastic modulus (GPa)	Poison's ratio	Shear modulus (GPa)	Density (kg/m^3)
Outer /Inner	Epoxy-E-Glass	6	E_1=45, E_2=E_3=10	υ_{12}= υ_{13}=0.3, υ_{23}=0.4	G_{12}=G_{13}=5, G_{23}=3.846	2000
core	PVC Foam	30	E=0.070	υ=0.3	G=0.027	60

Table 3: Material properties of the sandwich conical shell.

β (deg.)	n	Ω (rad/sec)=300		Ω (rad/sec)=600	
		m=1	m=2	m=1	m=2
15	3	379.49	389.12	399.66	409.22
	4	348.28	358.32	367.34	380.15
	5	330.93	342.79	348.70	361.61
	6	341.84	347.17	353.91	363.18
	7	352.73	361.20	371.42	379.05
30	3	476.78	491.86	642.01	678.77
	4	432.66	444.25	596.94	625.48
	5	417.70	431.63	579.27	600.82
	6	415.91	429.89	574.21	592.46
	7	421.42	437.04	586.39	607.08

Table 4: Convergence of frequencies (Hz) of backward wave for the rotating sandwich conical shell with simply supported boundary condition (L/r_1=3, h_c/r_1=0.1, h_o=h_i=h_c/5, (45/0/-45/$core$/-45/0/45)).

Since there is not any investigation in the literatures on the free vibration analysis of the rotating sandwich conical shells with flexible core and for further validation, the free vibration analysis of the rotating sandwich conical panel with a flexible core is carried out using ANSYS parametric design language software (Figure 3).

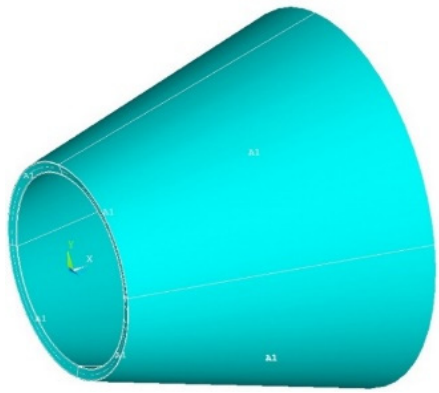

Figure 3: Geometrical modeling of the rotating sandwich conical shell with simply supported boundary conditions in ANSYS (h_c/r_1=0.1, L/r_1=3, h_c/h_f=5, (45/0/-45/*core*/-45/0/45)).

The layered structural elements shell 281 with eight nodes are applied to model the composite face sheets of the sandwich panel, and the higher order solid 186 elements with 20 nodes, are selected to model the flexible PVC foam core (Figure 4).

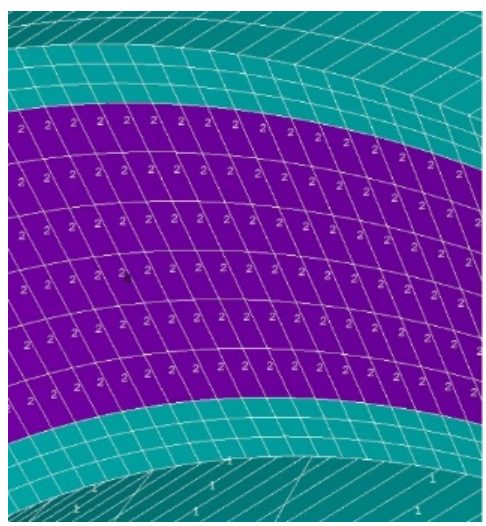

Figure 4: The finite element model of the conical sandwich shell in ANSYS representing the two used different element types.

In the modeling of sandwich structures, the correct finite element modeling and continuity conditions is obtained using of a set of user-defined constraint equations. For this purpose, two types of

face sheets with different fiber orientations have been considered. The material and geometry properties are presented in Table 5.

Layer	Materials	Thickness (mm)	Elastic modulus (GPa)	Poison's ratio	Shear modulus (GPa)	Density (kg/m^3)
Outer/ Inner	FRP	6	E_1=24.51, E_2=E_3=7.77	υ_{12}= υ_{13}=0.078, υ_{23}=0.49	G_{12}=G_{13}=3.34, G_{23}=1.34	1800
core	PVC Foam	30	E=0.10363	υ=0.33	G=0.039	130

Table 5: Material and geometric properties defining the conical sandwich shell used to assess the validation and convergence behavior of the present methodology in ANSYS.

In order to show the vibration modes of the rotating conical sandwich shell intuitively, Figure 5 gives some sample vibration mode shapes with several circumferential wave numbers. Table 6 shows that the results of the present study are in good agreement with the results of the present ANSYS model.

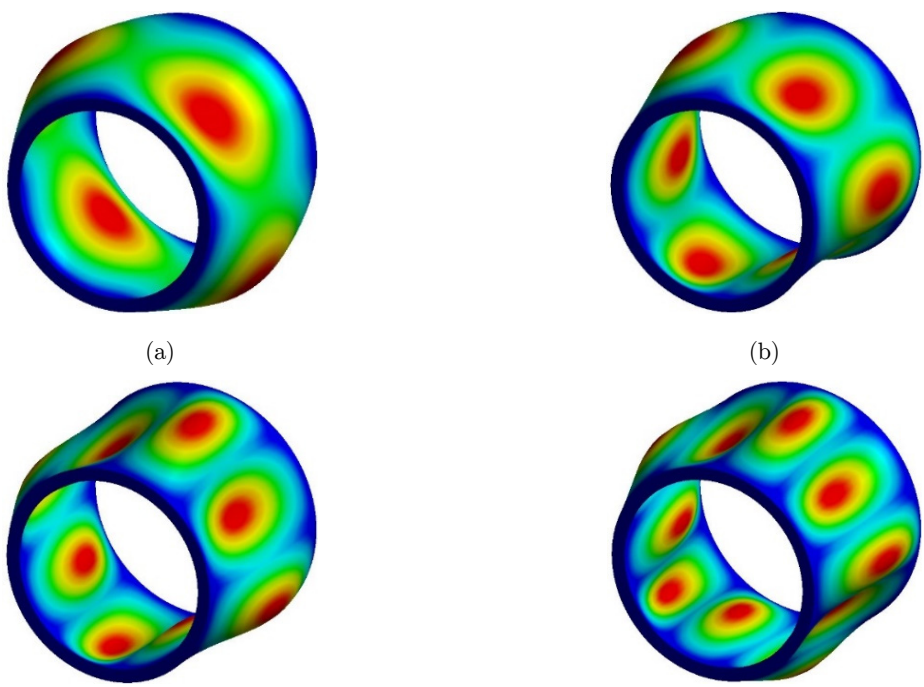

Figure 5: Some modes for the rotating conical sandwich shell with simply supported boundary condition for different circumferential wave numbers (m=1, h_c/r_1=0.1, L/r_1=3, h_c/h_f=5, (45/0/-45/core/-45/0/45)). (a) mode (1,4) (b) mode (1,6) (c) mode (1,8) (d) mode (1,10).

Material properties	n	Present	ANSYS	Discrepancy (%)	Present	Ansys	Discrepancy (%)
		ωb			ωf		
(0/90/0/ Core/ 0/90/0)	3	262.34	271.32	3.31	335.53	347.41	3.42
	4	238.61	245.18	2.68	314.29	322.48	2.54
	5	227.02	233.54	2.79	304.48	313.12	2.76
	6	224.78	229.22	1.94	302.93	309.05	1.98
(45/0/-45/ core/ -45/0/45)	3	311.67	321.90	3.18	351.70	362.76	3.05
	4	290.32	298.16	2.63	326.09	335.07	2.68
	5	282.06	289.32	2.51	316.40	324.25	2.42
	6	280.40	285.74	1.87	314.00	319.53	1.73

Table 6: Comparison of frequencies (Hz) of the rotating conical sandwich shell with simply supported boundary conditions (L/r_1=3, β=15°, h_c/r_1=0.1, m=1, Ω=300 *rad/sec*).

After displaying the good convergence rate and accuracy of the approach, some parametric studies for the frequencies of the rotating truncated conical sandwich with material properties shown in Table 3 and having simply supported boundary conditions are done. As a first example, the influences of the angular velocity on the frequencies of backward and forward waves for the rotating truncated conical sandwich shells are shown in Figure 6. It can be seen that, by increasing the angular velocity of rotation, the fundamental frequency of forward waves decreases for all the values of semi-vertex angles, whereas that of backward waves has direct relation with angular velocity. If both the Coriolis and centrifugal effects are considered, the natural frequencies of backward waves increase monotonically with the rotating speed, and those of forward waves decrease but if only the centrifugal effect is included, the natural frequencies of both the backward and forward waves increase monotonically and there is very Little difference between the natural frequencies of the two waves (Hua et al., 2005). It is observable from the Figure 6 that the angular velocity has significant effect on the frequencies of such structures. In larger cone angles, the diagram has a much greater slope. As can be seen, by increasing the angular velocity and cone angle, the difference between the frequency of backward and forward waves has grown. In velocity of 600 rad/s, for the semi-vertex angle 5°, value of the backward frequency is near that of the forward one while the ratio is more than 13 in both of them for the angle 60°. In a similar manner, in ref. (Hua et al., 2005), the backward frequencies of the rotating sandwich shell increase while the angular velocity rises; however, the forward frequencies firstly decrease and then, increase in cone angles more than 45°. Also, in larger cone angles, the backward and forward frequencies go far from each other by growing of the velocity.

In another part of investigations, the influence of the angular velocity, as an important parameter, on the fundamental frequencies of the rotating conical sandwich panel accompanied by converging rate of the method has been surveyed (Figure 7). It is obvious that the angular velocity has a direct effect on the frequencies of the backward wave, i.e., the frequency amount rises by increasing this parameter. However, as can be seen, the effect of circumferential wave number on the value of frequency is obvious. Also, in circumferential wave number between 4 and 6, the minimum value of frequency is achieved. Comparing the results with those of refs. (Civalek, 2006, Hua, 2000a, Hua et al., 2005) reveals that the frequency of backward waves in all the studies has a straight relation with angular velocity of rotation.

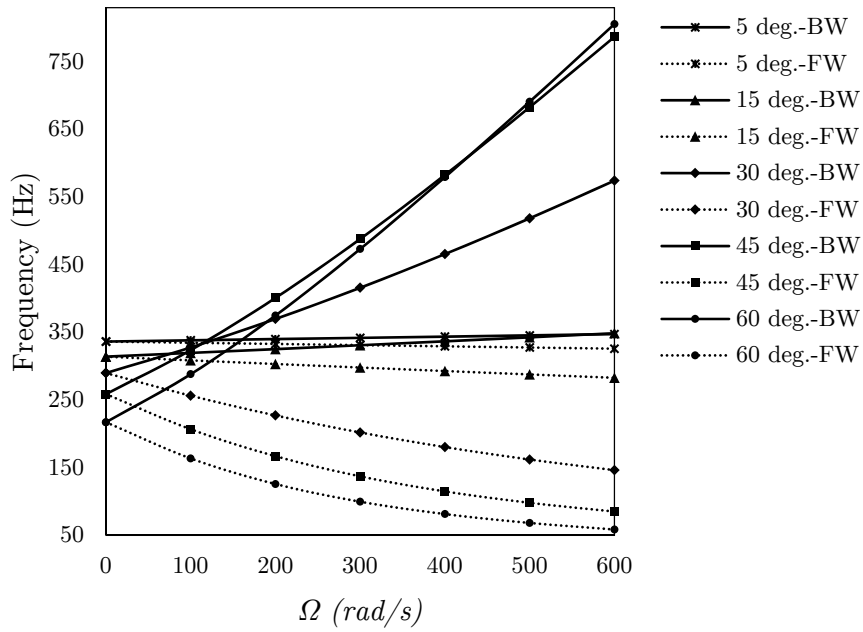

Figure 6: Relationship between the fundamental frequency of the forward and backward wave and rotating speed at various cone angles for a simply supported conical sandwich shell (m=1, h_c/r_1=0.1, L/r_1=3, h_c/h_f=5, (45/0/-45/*core*/-45/0/45)).

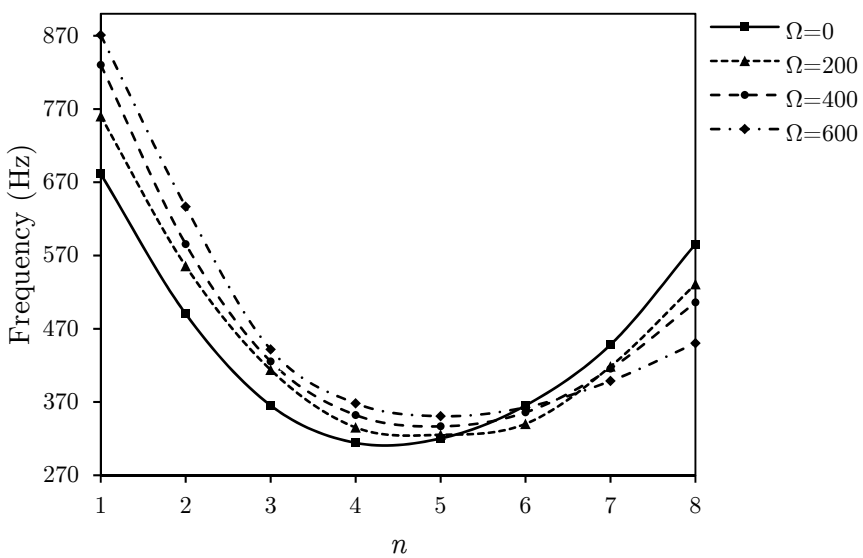

Figure 7: Relationship between the frequency of backward wave and circumferential wave number at various rotating speeds for a simply supported conical sandwich shell (m=1, h_c/r_1=0.1, L/r_1=3, h_c/h_f=5, β=15°, (45/0/-45/*core*/-45/0/45)).

As another research on geometry effects and convergence rate, the effect of the semi-vertex cone angle on the backward frequencies of the rotating sandwich conical shells for different values of the circumferential wave number has been examined and the results are presented in Figure 8. It can be seen that, at velocity of 300 rad/s for cone angles from 15° to 45°, the backward frequency increases by increasing the cone angle, but this routine defers for the cone angle values of 60° and 5°. It is obvious that the impact of the semi-vertex cone angle on the frequencies is very considerable. In refs. (Hua et al., 2005, Talebitooti, 2013), the backward frequency of the conical shell and the semi-vertex angle of the geometry have direct relationship with angles below 45°, as by increasing the angle from 45° to 60°, the frequency of the backward wave decreases.

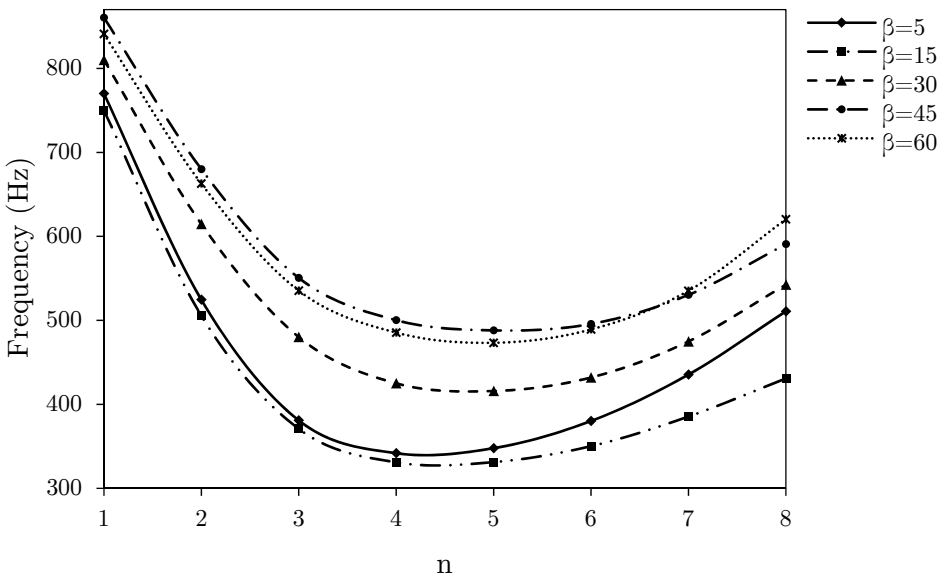

Figure 8: Relationship between the frequency of the backward wave and circumferential wave number at various semi-vertex cone angles for a simply supported conical sandwich shell (m=1, h_c/r_1=0.1, L/r_1=3, h_c/h_f=5, Ω=300rad/s, (45/0/-45/$core$/-45/0/45)).

The variations of the backward frequencies against the ratios of cone length to small-mean-radius and the core thickness to small-mean-radius of the rotating sandwich conical shells are presented in Figures 9 and 10, respectively, as the two important geometrical parameters for two different values of the angular velocity (Ω) For comparison and validation, the results of FEM have been shown.

Figure 9 shows that the length-to-small mean radius ratio has significant effect on the frequencies. This ratio also has a contrary effect on the backward frequency and as can be seen, the influence of this parameter is more important in smaller length-to-small mean radius ratios. For angular velocity of 600 rad/s, the slope in the smallest ratio is more than 29 times of that in the largest ratio and more than 8 for velocity of 300 rad/s. When the L/r_1 ratio is small, the decrease in the frequency with the L/r_1 ratio is rapid. With subsequent increase in the L/r_1 ratio, the decrease in the backward frequency with L/r_1 becomes relatively more gradual. Also, as can be seen in works by Hua et al. (2005) and Malekzadeh and Heydarpour (2013), the same trend is obvious, as by increasing this ratio

in a rotating sandwich type or simple conical shell, the frequencies of both the backward and forward waves decrease first rapidly and then, in a more gradual manner. Also, by increasing the angular velocity, the frequency of backward waves is growing.

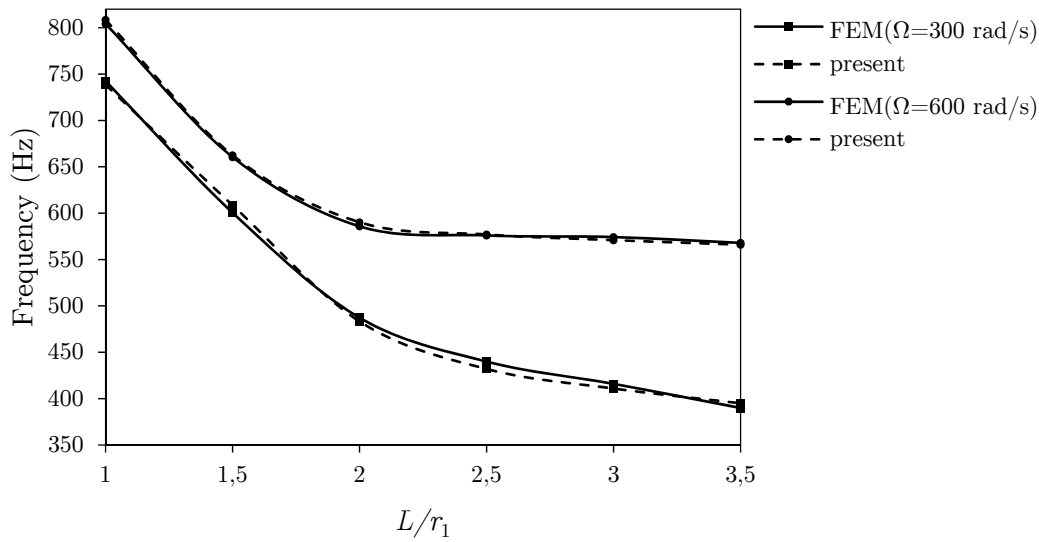

Figure 9: Relationship between the frequency of the backward wave and length-to-small mean radius ratio at two rotating speeds for a simply supported conical sandwich shell (m=1, h_c/r_1=0.1, h_c/h_f=5, β=30°, (45/0/-45/*core*/-45/0/45)).

In addition, the effects of core thickness-to-small mean radius ratio on the backward frequencies of rotating conical sandwich shell are presented for eleven ratios and two different angular velocities. Figure 10 shows that, by increasing the core thickness-to-small mean radius ratio, the backward frequency decreases for the ratios less than 1/15 and also for those more than 1/7.5, but increases for ratios between 1/15 and 1/7.5. This behavior is duplicated for the two different velocities, although as can be seen, the ascending and descending rate of frequency changing has a considerable grow up to twice by increasing the angular velocity. Hence, this geometrical parameter has considerable effect on the backward frequencies as the values of the ratio vary. In Hua et al. (2005), it is also observed that the increase in the frequency for both the backward and forward waves is very minimal with increasing the thickness to radius ratio. Also, it is observable from research done by Malekzadeh and Heydarpour (2013) that the more thickness-to-mean radius ratio is, the more frequency parameters becomes. The differences between the results of the previously mentioned researches and also the results obtained in the present work show that parameters such as boundary conditions, geometry of rotating structure, flexibility and material properties can affect this non-predictable behavior.

In Figure 11, the relation between the backward frequency and the ratio of core-to-face sheet thickness is investigated for twelve samples of this ratio and two different angular velocities. It is observed that the frequency slopes decline in ratio values from 1 to 3 and also more than 6, whereas they ascend in ratios between 3 and 6. As can be seen, the ascending and descending rate of frequency

changing has a considerable growth up to twice by increasing the angular velocity. This treatment is similar in different angular velocities. Also, as was shown previously and can be seen from Figure 9 to 11, the backward frequency rises with increasing the angular velocities.

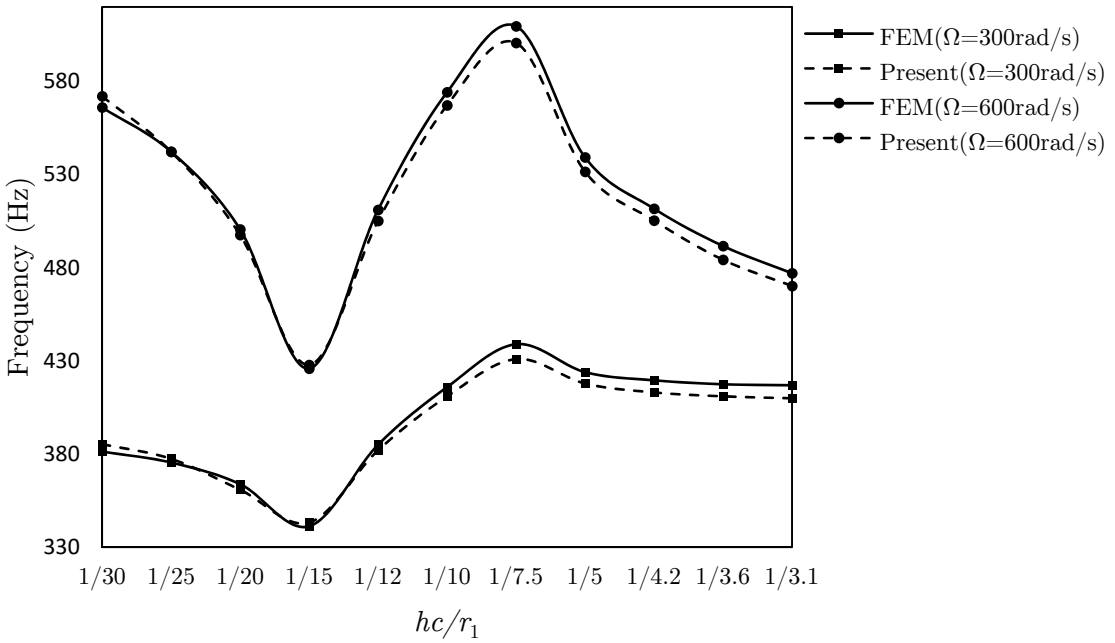

Figure 10: Relationship between the frequency of the backward wave and core thickness-to-small mean radius ratio at two rotating speeds for a simply supported conical sandwich shell (m=1, L/r_1=3, h_f/r_1=0.02, β=30°, (45/0/-45/*core*/-45/0/45)).

Finally, the effects of the semi-vertex cone angle on the backward and forward frequency of rotating conical sandwich for three different ratios of the length to small mean radius are presented for velocity value of 300 *rad/s*. As is clear in Figure 12, and also according to results shown in Figure 8, in cone angles lower than 15° and greater than 45°, the backward frequency decreases by rising the cone angle, but between these angles, it ascends by growing the slope of the angle. Besides, the L/r_1 ratio has a contrary effect on both the forward and backward frequencies, such that the frequencies decline by increasing the ratio. Again, in contrast with the backward frequency, the forward frequency declines with growth of the cone angle. Comparing the present results by those in ref. (Hua et al., 2005), it is clear that, except for the descending behavior of backward frequencies between angles 5° and 15°, the residual results of backward frequencies manners are the same in both the activities. However, forward frequency has a different trend, and increases by growing the angle. Oppositely, in refs. (Talebitooti, 2013, Malekzadeh and Heydarpour, 2013 and Heydarpour et al., 2014), in a similar manner with the present work, the frequency decreases with increasing the cone angle, although in refs. (Malekzadeh and Heydarpour, 2013, Heydarpour et al., 2014), the authors do not mention backward or forward frequencies clearly. It can be due to difference in geometrical parameters, material isotropy and flexibility, and mode number or the range of velocities given in that work.

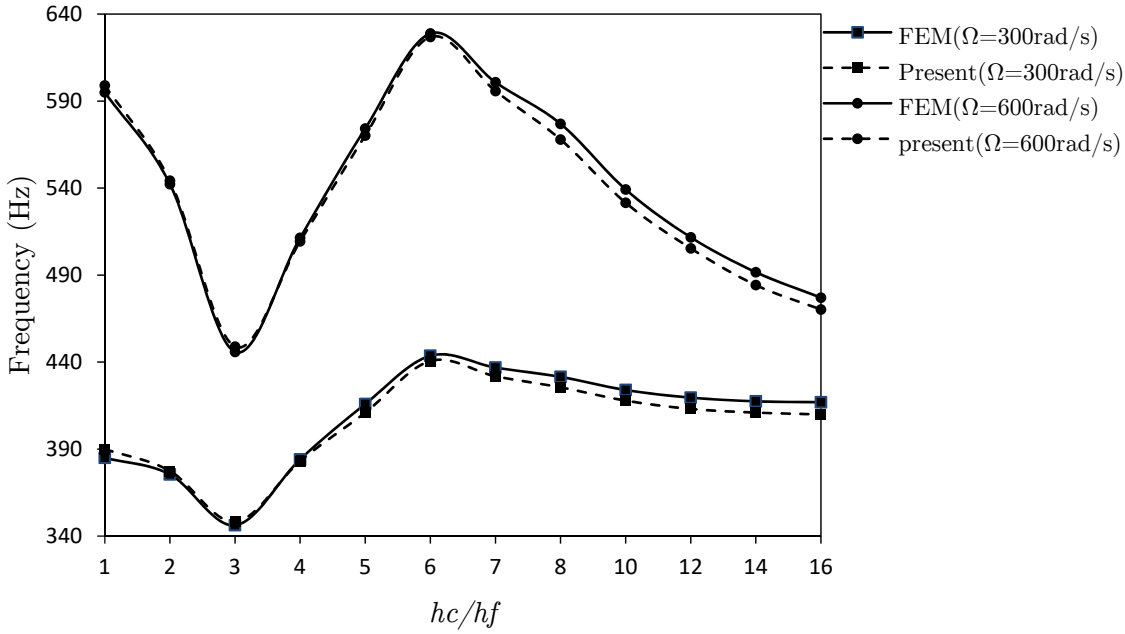

Figure 11: Relationship between the frequency of the backward wave and core thickness-to-face sheet thickness ratio at two rotating speeds for a simply supported conical sandwich shell (m=1, L/r_1=3, β=30°, (45/0/-45/*core*/-45/0/45)).

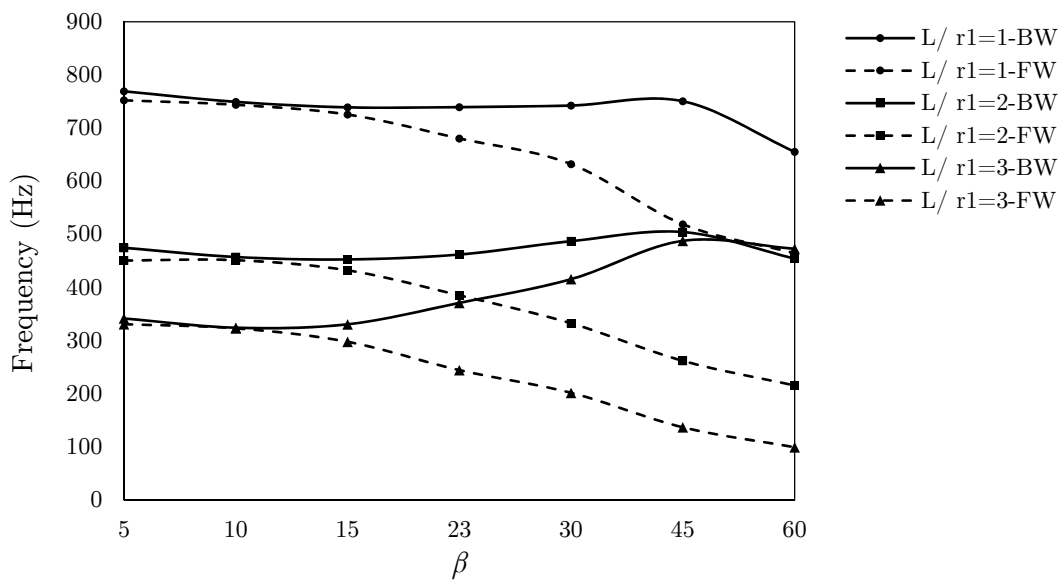

Figure 12: Relationship between the frequency of the backward and forward wave and semi-vertex cone angle at three different length-to-radius ratios for a simply supported conical sandwich shell (m=1, h_c/r_1=0.1, h_c/h_f=5; **Ω**=300 *rad/s*, (45/0/-45/*core*/-45/0/45)).

6 CONCLUSION

Free vibration response of the rotating sandwich truncated conical shells was investigated for the first time based on an improved high-order shear deformable theory of sandwich panels with laminated composite face sheets and a homogenous soft core، considering the effect of thickness to radius of the curvature ratio. By considering the centrifugal and Coriolis accelerations as well as the initial hoop tension, the free vibration equations of motion were derived based on the Hamilton's principle. The Galerkin's method accompanied by trigonometric double Fourier series which satisfy the boundary conditions, as an efficient and accurate method, was employed to reduce the governing partial differential equations system to an ordinary one. Then by solving the eigenvalue problem analytically, convergence rate of the approach was shown and its accuracy with small computational efforts was displayed.

One sees that the minimum value of the frequency can happen for a circumferential wave number more than (n=4). It was concluded that, the circumferential wave number, angular velocity, semi-vertex cone angle, length-to-small mean radius and thickness-to-small mean radius ratios have significant effects on the frequencies of the rotating sandwich conical shells. Based on the presented numerical results, the following conclusions can be made:

- By increasing the angular velocity of the rotating conical sandwich panel, the frequencies of the backward waves increase for different values of the semi-vertex angles while those of the forward waves decrease for all cone angles. In velocity of 600 rad/s, for semi-vertex angle 5°, the value of the backward frequency is near the value of the forward frequency while their ratio is more than 13 for angle 60°.
- For angular velocities between 200 and 400 *rad/s* and semi-vertex angles less than 15° and more than 45°, the semi-vertex angle has a contrary effect on the backward frequency, i.e., the backward frequency is reduced by increasing this parameter while the relationship between the cone angle and forward frequency of the rotating conical sandwich is straight.
- The length-to-small mean radius ratio has significant effects on the frequency, and by increasing this ratio, the frequencies of the forward and backward waves decrease. For angular velocity of 600 rad/s, the slope in the smallest ratio is more than 29 times of that in the largest ratio and is more than 8 for velocity of 300 rad/s. When the L/r_1 ratio is small, the decrease in the frequency with the L/r_1 ratio is rapid. With subsequent increase in the L/r_1 ratio, the decrease in the backward frequency with L/r_1 becomes relatively more gradual.
- The core thickness-to-small mean radius ratio has considerable effects on the frequency of the rotating sandwich, and by increasing this ratio up to around 1/15 and more than 1/7.5, the backward frequency decreases. In ratios between 1/15 and 1/7.5, the frequency of the backward wave increases. The ascending and descending rate of frequency changing has a considerable growth (up to twice) by increasing the angular velocity.
- The dependency of frequency is noticeable on the core-to-face sheet thickness ratio. For the ratios between 3 and 6, their relationship is almost linear with rising the slope.

References

Amabili, M., Reddy, J.N., (2010). A new non-linear higher-order shear deformation theory for large-amplitude vibrations of laminated doubly curved shells, Int. J. Non Linear Mech. 45(4): 409–418.

Amabili, M., (2013). A new nonlinear higher-order shear deformation theory with thickness variation for large-amplitude vibrations of laminated doubly curved shells, J. of Sound and vibration 332(19): 4620–4640.

ANSYS Documentation, (2016). http://www.ansys.com.

Bacon, M.D., Bert, C.W., (1962). Unsymmetric free vibrations of orthotropic sandwich shells of revolution, *AIAA* J. 5(3): 413.

Bardell, N.S., Langley, R.S., Dunsdon, J.M., Aglietti, G.S., (1999). An h-p finite element vibration analysis of open conical sandwich panels and conical sandwich frusta, J. of Sound and vibration 226(2): 345-377.

Bert, C.W., Ray, J.D., (1969). Vibrations of orthotropic sandwich conical shells with free edges, Int. J. mech. Sci. 11: 767.

Carrera, E., Brischetto, S.A., (2009). A comparison of various kinematic models for sandwich shell panels with soft core, Journal of Composite Materials 43(20): 2201-2221.

Chen, Y., Zhao, H.B., Chen, Z.P., Grieger, I., Kröplin, B.H., (1993). Vibration of high speed rotating shells with calculations for cylindrical shells, J. of Sound and Vibration 160: 137–160.

Chen, C., Dai, L., (2009). Nonlinear vibration and stability of a rotary truncated conical shell with intercoupling of high and low order modals, Communications in Nonlinear Science and Numerical Simulation 14: 254–269.

Chen, C., (2012). Nonlinear dynamic of a rotating truncated conical shell, Nonlinear Approaches in Engineering Applications, Springer, New York.

Civalek, O., (2006). An efficient method for free vibration analysis of rotating truncated conical shells, Int. J. Press. Vess. Pip. 83: 1–12.

Dey, S., Karmakar, A., (2012). Frequencies of delaminated composite rotating conical shells—a finite element approach, Finite Elem. Anal. Des. 56: 41–51.

Frostig, Y., Baruch, M., Vilnay, O., Sheinman, I., (1992). High-order theory for sandwich beam behavior with transversely flexible core, J. Eng. Mech. 118(5): 1026–43.

Frostig, Y., Thomsen, O.T., (2004). High-order free vibration of sandwich panels with a flexible core, Int. J. of Solids and Struct. 41: 1697–1724.

Gupta, A.P., Jain, M., (1978). Axisymmetric vibrations of conical sandwich shells, Department of Math., University of Roorke, Roorke, pp.1322-1336.

Han, Q., Chu, F., (2013). Parametric instability of a rotating truncated conical shell subjected to periodic axial loads, Mechanics Research Communications 53: 63–74.

Han, Q., Chu, F., (2014). Parametric resonance of truncated conical shells rotating at periodically varying angular speed, J. of Sound and Vibration 333: 2866–2884.

Heydarpour, Y., Aghdam, M.M., Malekzadeh, P., (2014). Free vibration analysis of rotating functionally graded carbon nanotube-reinforced composite truncated conical shells, Composite Structures 117: 187-200.

Hua, L., (2000a). Frequency analysis of rotating truncated circular orthotropic conical shells with different boundary conditions, Compos. Sci. Tech. 60: 2945–2955.

Hua, L., (2000b). Frequency characteristics of a rotating truncated circular layered conical shell, Compos. Struct. 50: 59–68.

Hua, L., (2000c). Influence of boundary conditions on the free vibrations of rotating truncated circular multi-layered conical shells, Compos. Part B Eng. 31: 265–75.

Hua, L., Lam, K.Y., (2000). The generalized differential quadrature method for frequency analysis of a rotating conical shell with initial pressure, Int. J. for Numerical Methods in Engineering 48: 1703–1722.

Hua, L., Lam, K.Y., (2001). Orthotropic influence on frequency characteristics of a thin rotating composites laminated conical shell using the generalized differential quadrature method, Int. J. Solids Struct. 38: 3995–4015.

Hua, L., Lam, K.Y., Ng, T.Y., (2005). Rotating shell dynamics, Elsevier Science, London.

Ji, W., Waas, A.M., (2010). 2D elastic analysis of the sandwich panel buckling problem: benchmark solutions and accurate finite element formulations, ZAMP 6: 897-917.

Kant, T., Swaminathan, K., (2002). Analytical solutions for the static analysis of laminated composite and sandwich plates based on a higher order refined theory, Compos. Struct. 56: 329-344.

Kardomateas, G.A., (2005). Wrinkling of wide sandwich panels/beams with orthotropic phases by an elasticity approach, J. Appl. Mech. 72: 818-825.

Korjakin, A., Rikards, R., Altenbach, H., Chate, A., (2001). Free damped vibrations of sandwich shells of revolution, J. of Sandwich Structures and Materials 3: 171-196.

Lam, K.Y., Hua, L., (1997). Vibration analysis of a rotating truncated circular conical shell, Int. J. Solids Struct. 34: 2183–2197.

Lam, K.Y., Hua, L., (1999a). Influence of boundary conditions on the frequency characteristics of a rotating truncated circular conical shell, J. of Sound and Vibration 223(2): 171–195.

Lam, K.Y., Hua, L., (1999b). On free vibration of a rotating truncated circular orthotropic conical shell, Composites Part B 30(2): 135–144.

Lam, K.Y., Hua, L., (2000). Influence of initial pressure on frequency characteristics of a rotating truncated circular conical shell, International Journal of Mechanical Sciences 42: 213–236.

Malekzadeh, K., Khalili, M.R., Mittal, R.K., (2005). Local and global damped vibrations of plates with a viscoelastic soft flexible core: an improved high-order approach, J. Sandwich Struct. Mater 7: 431–456.

Malekzadeh, P., Heydarpour, Y., (2013). Free vibration analysis of rotating functionally graded truncated conical shells, Compos. Struct. 97: 176–188.

Malekzadeh, K., Livani, M., (2015). The buckling of truncated conical sandwich panels under axial compression and external pressure, J. Mech. Eng. Sci. 229 (11): 1965–1978.

Matsunaga, H., (2005). Thermal buckling of cross-ply laminated composite and sandwich plates according to a global higher-order deformation theory, Compos. Struct. 68: 439-454.

Mozaffari, A., Morovat, F., (2015). Analytical solution for buckling of composite sandwich truncated conical shells subject to combined external pressure and axial compression load, Int. J. Advanced Design and Manufacturing Technology 8(4): 83-94.

Nayak, A.K., Shenoi, R.A., Moy, S.S.J., (2006). Dynamic response of composite sandwich plates subjected to initial stresses, Composites: Part-A 37: 1189-1205.

Ng, T.Y., Hua, L., Lam, K.Y., (2003). Generalized differential quadrature for free vibration of rotating composite laminated conical shell with various boundary conditions, Int. J. Mech. Sci. 45: 567–587.

Noor, A.K., Burton, W.S., Bert, C.W., (1996). Computational models for sandwich panels and shells, Applied Mechanics Reviews 49: 155-199.

Qinkai, H., Fulei, C., (2013). Effect of rotation on frequency characteristics of a truncated circular conical shell, Arch. Appl. Mech. 83: 1789–1800.

Ramesh, T.C., Ganesan, N., (1994). Finite element analysis of conical shells with a constrained viscoelastic layer, J. of Sound and Vibration 171(5): 577–601.

Reddy J.N., (2004). Mechanics of laminated composite plates and shells, Theory and Analysis, second ed., CRC Press, New York.

Seidi, J., Khalili, S.M.R., Malekzadeh, K., (2015). Temperature-dependent buckling analysis of sandwich truncated conical shells with FG face sheets, Composite Structures 131: 682–691.

Shariyat, M., (2012). A general nonlinear global-local theory for bending and buckling analyses of imperfect cylindrical laminated and sandwich shells under thermomechanical loads. Meccanica 47: 301–319.

Sharnappa, S., Ganesan, N., Sethuraman, R. (2009). Free vibration analysis of truncated sandwich conical shells with constrained electro-rheological fluid damping, 8th Int. conf. on Vibration Problems (ICOVP07), Springer Proceedings in Physics, Springer Netherlands 126: 357.

Sivadas, K.R., (1995). Vibration analysis of pre-stressed rotating thick circular conical shell, J. of Sound and Vibration 186: 99–109.

Talebitooti, M., Ghayour, M., Ziaei-Rad, S., Talebitooti, R., (2010). Free vibrations of rotating composite conical shells with stringer and ring stiffeners, Arch. Appl. Mech. 80: 201–215.

Talebitooti, M., (2013). Three-dimensional free vibration analysis of rotating laminated conical shells: layerwise differential quadrature (LW-DQ) method, Arch. Appl. Mech. 83: 765–781.

Wilkins, D.J., Bert, C.W., Egle, D.M., (1970). Free vibrations of orthotropic sandwich conical shells with various boundary conditions, J. of Sound and vibration 13: 211-228.

Zhong, C., Reimerdes, H.G., (2007). Stability behavior of cylindrical and conical sandwich shells with flexible core, J. of Sandwich Structures and Materials 9: 143–166.

APPENDIX I

$$
\begin{aligned}
&K(1,1) = R_\theta^j(Ar_{11} + \frac{4}{{h_c}^4}(2G_{R4} + \lambda_{R4} + \frac{2}{h_c}(2G_{R5} + \lambda_{R5})) + \frac{8}{{h_c}^5}(2G_{R5} + \lambda_{R5} + \frac{2}{h_c}(2G_{R6} + \lambda_{R6})))u_{0o,ss}\\
&+\frac{1}{\cos\beta}(\bar{A}_{66} + \frac{4}{{h_c}^4}(G_{\Gamma4} + \frac{2}{h_c}G_{\Gamma5}) + \frac{8}{{h_c}^5}(G_{\Gamma5} + \frac{2}{h_c}G_{\Gamma6}))u_{0o,\theta\theta} + \frac{1}{\cos\beta}A_{16}(u_{0o,s\theta} + u_{0o,\theta s})\\
&+\tan\beta(Ar_{11} - \frac{1}{R_\theta^j}B_{11} + \frac{4}{{h_c}^4}(\lambda_4 + \frac{2}{h_c}\lambda_5 - \frac{1}{R_\theta^c}(2G_5 + \lambda_5 + \frac{2}{h_c}(2G_6 + \lambda_6))\\
&+\frac{4}{{h_c}^4}(2G_{R4} + \lambda_{R4} + \frac{2}{h_c}(2G_{R5} + \lambda_{R5})) - \frac{4}{{h_c}^4}(\lambda_4 + \frac{2}{h_c}\lambda_5) + \frac{8}{{h_c}^5}(\lambda_5 + \frac{2}{h_c}\lambda_6 - \frac{1}{R_\theta^c}(2G_6 + \lambda_6 + \frac{2}{h_c}(2G_7 + \lambda_7)))\\
&+\frac{8}{{h_c}^5}(2G_{R5} + \lambda_{R5} + \frac{2}{h_c}(2G_{R6} + \lambda_{R6})) - \frac{8}{{h_c}^5}(\lambda_5 + \frac{2}{h_c}\lambda_6))u_{0o,s}\\
&+(I_0^j\,\Omega^2\sin^2\beta + \frac{4\Omega^2\sin^2\beta}{{h_c}^4}(I_4^c + \frac{4}{h_c}I_5^c + \frac{4}{{h_c}^2}I_6^c) - sin\beta\tan\beta\bar{A}_{22} - \frac{16R_\theta^c}{{h_c}^4}(G_{R2} + \frac{3}{h_c}G_{R3})\\
&-\frac{48R_\theta^c}{{h_c}^5}(G_{R3} + \frac{3}{h_c}G_{R4}) + (\frac{8\tan^2\beta}{{h_c}^5R_\theta^c} - \frac{4\tan^2\beta}{{h_c}^3R_\theta^c})(\lambda_5 + \frac{2}{h_c}\lambda_6) - \frac{4\sin\beta\tan\beta}{{h_c}^4}(2G_{\Gamma4} + \lambda_{\Gamma4} + \frac{2}{h_c}(2G_{\Gamma5} + \lambda_{\Gamma5})\\
&-\frac{4\sin\beta\tan\beta}{{h_c}^3}(2G_{\Gamma5} + \lambda_{\Gamma5} + \frac{2}{h_c}(2G_{\Gamma6} + \lambda_{\Gamma6})))u_{0o}
\end{aligned}
\tag{A-1}
$$

$$
M(1,1) = -(\mathrm{I}_0^j + \frac{4}{{h_c}^4}(I_4^c + \frac{4}{h_c}I_5^c + \frac{4}{{h_c}^2}I_6^c))\ddot{u}_{0o}
$$

$$
\begin{aligned}
&K(1,3) = +(R_\theta^j Ar_{16} + Br_{16})v_{0j,ss} + \frac{1}{\cos\beta}(\bar{A}_{26} + \frac{1}{R_\theta^j}\bar{B}_{26})v_{0j,\theta\theta} + \frac{1}{\cos\beta}(A_{66} + \frac{1}{R_\theta^j}B_{66})v_{0j,s\theta}\\
&+\frac{1}{\cos\beta}(A_{12} + \frac{1}{R_\theta^j}B_{12} + \frac{2(2R_\theta^o - h_o)}{R_\theta^o{h_c}^4}(\lambda_4 + \frac{2}{h_c}\lambda_5) + \frac{4(2R_\theta^o - h_o)}{R_\theta^o{h_c}^5}(\lambda_5 + \frac{2}{h_c}\lambda_6))v_{0o,\theta s}\\
&-\tan\beta(A_{16} + A_{26} - Ar_{16} + \frac{1}{R_\theta^j}(2B_{16} + B_{26} + \frac{1}{R_\theta^j}D_{16}))v_{0j,s}\\
&+\tan\beta(-(\bar{A}_{22} + \bar{A}_{66} + \frac{1}{R_\theta^j}(\bar{B}_{22} + \bar{B}_{66} + \frac{1}{R_\theta^j\cos\beta}B_{12})) + \frac{2h_o}{R_\theta^o 2{h_c}^4\cos\beta}(\lambda_4 + \frac{2}{h_c}\lambda_5)\\
&-\frac{2(2R_\theta^o - h_o)}{R_\theta^o{h_c}^4}(G_{\Gamma4} + \frac{2}{h_c}G_{\Gamma5}) - \frac{4(2R_\theta^o - h_o)}{R_\theta^o{h_c}^5}(G_{\Gamma5} + \frac{2}{h_c}G_{\Gamma6}) + \frac{4h_o}{R_\theta^{o2}{h_c}^5\cos\beta}(\lambda_5 + \frac{2}{h_c}\lambda_6)\\
&-\frac{2(2R_\theta^o - h_o)}{R_\theta^o{h_c}^4}(2G_{\Gamma4} + \lambda_{\Gamma4} + \frac{2}{h_c}(2G_{\Gamma5} + \lambda_{\Gamma5})) - \frac{4(2R_\theta^o - h_o)}{R_\theta^o{h_c}^5}(2G_{\Gamma5} + \lambda_{\Gamma5} + \frac{2}{h_c}(2G_{\Gamma6} + \lambda_{\Gamma6})))v_{0o,\theta}
\end{aligned}
$$

$$+sin\beta\tan\beta(\overline{A}_{26}+\frac{1}{R_\theta^j}(\overline{B}_{26}+\frac{1}{R_\theta^j\cos\beta}B_{16}))v_{0j}$$

$$C(1,3)=+2\Omega\sin\beta(\mathrm{I}_0^j+\frac{1}{R_\theta^j}\mathrm{I}_1^j+\frac{2(2R_\theta^o-h_o)}{R_\theta^o{h_c}^4}(I_4^c+\frac{4}{h_c}I_5^c+\frac{4}{{h_c}^2}I_6^c))\dot{v}_{0o}$$

$$K(11,1)=(+\frac{2R_\theta^c}{{h_c}^2}(2G_{R2}+\lambda_{R2}+\frac{2}{h_c}(2G_{R3}+\lambda_{R3}))-\frac{8R_\theta^c}{{h_c}^4}(2G_{R4}+\lambda_{R4}+\frac{2}{h_c}(2G_{R5}+\lambda_{R5})))u_{0o,ss}$$
$$+(\frac{2}{{h_c}^2\cos\beta}(G_{\Gamma2}+\frac{2}{h_c}G_{\Gamma3})-\frac{8}{{h_c}^4\cos\beta}(G_{\Gamma4}+\frac{2}{h_c}G_{\Gamma5}))u_{0o,\theta\theta}$$
$$+(\frac{2\tan\beta}{{h_c}^2}(\lambda_2+\frac{2}{h_c}\lambda_3-\frac{1}{R_\theta^c}(2G_3+\lambda_3+\frac{2}{h_c}(2G_4+\lambda_4)))-\frac{8\tan\beta}{{h_c}^4}(\lambda_4+\frac{2}{h_c}\lambda_5-\frac{1}{R_\theta^c}(2G_5+\lambda_5+\frac{2}{h_c}(2G_6+\lambda_6)))$$
$$+\frac{2\tan\beta}{{h_c}^2}(2G_{R2}+\lambda_{R2}+\frac{2}{h_c}(2G_{R3}+\lambda_{R3}))-\frac{8\tan\beta}{{h_c}^4}(2G_{R4}+\lambda_{R4}+\frac{2}{h_c}(2G_{R5}+\lambda_{R5}))$$
$$-\frac{2\tan\beta}{{h_c}^2}(\lambda_2+\frac{2}{h_c}\lambda_3)+\frac{8\tan\beta}{{h_c}^4}(\lambda_4+\frac{2}{h_c}\lambda_5))u_{0o,s}$$
$$+(-\frac{2\sin\beta\tan\beta}{{h_c}^2}(2G_{\Gamma2}+\lambda_{\Gamma2}+\frac{2}{h_c}(2G_{\Gamma3}+\lambda_{\Gamma3}))+\frac{8\sin\beta\tan\beta}{{h_c}^4}(2G_{\Gamma4}+\lambda_{\Gamma4}+\frac{2}{h_c}(2G_{\Gamma5}+\lambda_{\Gamma5}))$$
$$+\frac{32R_\theta^c}{{h_c}^4}(G_{R2}+\frac{3}{h_c}G_{R3})+\frac{2\Omega^2\sin^2\beta}{{h_c}^2}(I_2^c+\frac{2}{h_c}I_3^c-\frac{4}{{h_c}^2}(I_4^c+\frac{2}{h_c}I_5^c)))u_{0o}$$

$$M(11,1)=-\frac{2}{{h_c}^2}(I_2^c+\frac{2}{h_c}I_3^c-\frac{4}{{h_c}^2}(I_4^c+\frac{2}{h_c}I_5^c))\ddot{u}_{0o}$$

$$K(11,3)=+\frac{(2R_\theta^o-h_o)}{{h_c}^2R_\theta^o\cos\beta}(\lambda_2+\frac{2}{h_c}\lambda_3-\frac{4}{{h_c}^2}(\lambda_4+\frac{2}{h_c}\lambda_5))v_{0o,\theta s}$$
$$+\frac{\tan\beta}{{h_c}^2R_\theta^{o2}}(\frac{h_o}{\cos\beta}(\lambda_2+\frac{2}{h_c}\lambda_3)-\frac{4h_o}{{h_c}^2\cos\beta}(\lambda_4+\frac{2}{h_c}\lambda_5)$$
$$-R_\theta^o(2R_\theta^o-h_o)(2G_{\Gamma2}+\lambda_{\Gamma2}+\frac{2}{h_c}(2G_{\Gamma3}+\lambda_{\Gamma3}))-R_\theta^o(2R_\theta^o-h_o)(G_{\Gamma2}+\frac{2}{h_c}G_{\Gamma3})$$
$$+\frac{4R_\theta^o(2R_\theta^o-h_o)}{{h_c}^2}(2G_{\Gamma4}+\lambda_{\Gamma4}+\frac{2}{h_c}(2G_{\Gamma5}+\lambda_{\Gamma5}))+\frac{4R_\theta^o(2R_\theta^o-h_o)}{{h_c}^2}(G_{\Gamma4}+\frac{2}{h_c}G_{\Gamma5}))v_{0o,\theta}$$

$$C(11,3)=\frac{2\Omega\sin\beta(2R_\theta^o-h_o)}{{h_c}^2R_\theta^o}(I_2^c+\frac{2}{h_c}I_3^c-\frac{4}{{h_c}^2}(I_4^c+\frac{2}{h_c}I_5^c))\dot{v}_{0o}$$

$$K(13,5)=$$
$$+(\frac{1}{h_c}(2G_{\Gamma1}+\lambda_{\Gamma1}+\frac{1}{\cos\beta}\lambda_0+\frac{2}{h_c}(2G_{\Gamma2}+\lambda_{\Gamma2}+\frac{2}{\cos\beta}\lambda_1))$$
$$+\frac{1}{R_\theta^ch_c}(2G_{\Gamma2}+\lambda_{\Gamma2}+\frac{1}{\cos\beta}\lambda_1+\frac{2}{h_c}(2G_{\Gamma3}+\lambda_{\Gamma3}+\frac{2}{\cos\beta}\lambda_2))$$

$$-\frac{4}{{h_c}^3}(2G_{\Gamma 3}+\lambda_{\Gamma 3}+\frac{1}{\cos\beta}\lambda_2+\frac{2}{h_c}(2G_{\Gamma 4}+\lambda_{\Gamma 4}+\frac{2}{\cos\beta}\lambda_3))$$
$$-\frac{4}{R_\theta^c {h_c}^3}(2G_{\Gamma 4}+\lambda_{\Gamma 4}+\frac{1}{\cos\beta}\lambda_3+\frac{2}{h_c}(2G_{\Gamma 5}+\lambda_{\Gamma 5}+\frac{2}{\cos\beta}\lambda_4))$$
$$+\frac{8R_\theta^c}{{h_c}^3}(G_{\Gamma 2}+\frac{2}{h_c}G_{\Gamma 3})+\frac{8}{{h_c}^3}(G_{\Gamma 3}+\frac{2}{h_c}G_{\Gamma 4})+\frac{8}{R_\theta^c {h_c}^3}(G_{\Gamma 4}+\frac{2}{h_c}G_{\Gamma 5}))w_{0o,\theta}$$

$$C(13,5)=-\frac{2\Omega\cos\beta}{h_c}(I_1^c+(\frac{1}{R_\theta^c}+\frac{2}{h_c})I_2^c+(\frac{2}{R_\theta^c h_c}-\frac{4}{{h_c}^2})I_3^c-(\frac{8}{{h_c}^3}+\frac{4}{R_\theta^c {h_c}^2})I_4^c-\frac{8}{R_\theta^c {h_c}^3}I_5^c)\dot{w}_{0o}$$

$$K(15,15)=+\tan\beta((G_{R0}-\frac{4}{{h_c}^2}G_{R2})-\frac{4}{{h_c}^2}(G_{R2}-\frac{4}{{h_c}^2}G_{R4})-\frac{1}{R_\theta^c}(G_1-\frac{4}{{h_c}^2}G_3)+\frac{4}{{h_c}^2 R_\theta^c}(G_3-\frac{4}{{h_c}^2}G_5))w_{0,s}^c$$
$$+R_\theta^c((G_{R0}-\frac{4}{{h_c}^2}G_{R2})-\frac{4}{{h_c}^2}(G_{R2}-\frac{4}{{h_c}^2}G_{R4}))w_{0,ss}^c+\frac{1}{\cos\beta}((G_{\Gamma 0}-\frac{4}{{h_c}^2}G_{\Gamma 2})-\frac{4}{{h_c}^2}(G_{\Gamma 2}-\frac{4}{{h_c}^2}G_{\Gamma 4}))w_{0,\theta\theta}^c$$
$$+(\frac{8R_\theta^c}{{h_c}^2}(\cos\beta\lambda_{\Gamma 1}-\frac{4}{{h_c}^2}(2\lambda_2+4G_2+\cos\beta\lambda_{\Gamma 3}))+\frac{8}{{h_c}^2}(\cos\beta\lambda_{\Gamma 2}-\frac{4}{{h_c}^2}(2\lambda_3+4G_3+\cos\beta\lambda_{\Gamma 4}))$$
$$-\cos\beta(2G_{\Gamma 0}+\lambda_{\Gamma 0}-\frac{4}{{h_c}^2}(2G_{\Gamma 2}+\lambda_{\Gamma 2}+\frac{2}{\cos\beta}\lambda_1))+\frac{4\cos\beta}{{h_c}^2}(2G_{\Gamma 2}+\lambda_{\Gamma 2}-\frac{4}{{h_c}^2}(2G_{\Gamma 4}+\lambda_{\Gamma 4}+\frac{2}{\cos\beta}\lambda_3))$$
$$+\Omega^2\cos^2\beta(I_0^c-\frac{8}{{h_c}^2}I_2^c+\frac{16}{{h_c}^4}I_4^c))w_0^c$$

$$M(15,15)=-(I_0^c-\frac{8}{{h_c}^2}I_2^c+\frac{16}{{h_c}^4}I_4^c)\ddot{w}_0^c$$

where

$$\begin{aligned}
G_k &= \int_{-h_c/2}^{h_c/2} G^c(z_c)\times\left(z_c\right)^k dz_c && , \quad k=0-6\\
G_{Rk} &= \int_{-h_c/2}^{h_c/2} G^c(z_c)\times\left(z_c\right)^k (1+\frac{z_c}{R_\theta^c})dz_c && , \quad k=0-6\\
G_{\Gamma k} &= \int_{-h_c/2}^{h_c/2} G^c(z_c)\times\left(z_c\right)^k \frac{1}{\Gamma_c} dz_c && , \quad k=0-6\\
G_{2\Gamma k} &= \int_{-h_c/2}^{h_c/2} G^c(z_c)\times\left(z_c\right)^k \frac{1}{{\Gamma_c}^2} dz_c && , \quad k=0-3\\
\lambda_k &= \int_{-h_c/2}^{h_c/2} \lambda^c(z_c)\times\left(z_c\right)^k dz_c && , \quad k=0-6\\
\lambda_{Rk} &= \int_{-h_c/2}^{h_c/2} \lambda^c(z_c)\times\left(z_c\right)^k (1+\frac{z_c}{R_\theta^c})dz_c && , \quad k=0-6
\end{aligned} \tag{A-2}$$

$$\lambda_{\Gamma k} = \int_{-h_c/2}^{h_c/2} \lambda^c(z_c) \times \left(z_c\right)^k \frac{1}{\Gamma_c} dz_c \qquad , \qquad k = 0-6$$

$$\lambda_{2\Gamma k} = \int_{-h_c/2}^{h_c/2} \lambda^c(z_c) \times \left(z_c\right)^k \frac{1}{{\Gamma_c}^2} .dz_c \qquad , \qquad k = 0-3$$

$$I_L^j = \sum_{k=1}^{n} \int_{Z_k}^{Z_{k+1}} \rho_j . z_j^L (R_\theta^j + z_j) dz_j \qquad , \qquad L = 0...6$$

$$\Gamma_j = \left({R_\theta}^j + z_j\right) cos\beta \qquad , \qquad j = o, i, c$$